

*Experimental Assessment  
of Air Permeability  
in a Concrete Shear Wall Subjected  
to Simulated Seismic Loading*

*Steven P. Girrens  
Charles R. Farrar*



**MASTER**

Los Alamos National Laboratory  
Los Alamos, New Mexico 87545

DISTRIBUTION OF THIS DOCUMENT IS UNLIMITED

## CONTENTS

ABSTRACT.....	1
I. INTRODUCTION.....	2
II. LITERATURE REVIEW.....	3
III. CONCRETE AIR PERMEABILITY, CAP-1, MODEL CONSTRUCTION.....	6
IV. AIR PERMEABILITY TESTING.....	12
V. COMPARISON OF PERMEABILITY DATA WITH PUBLISHED RESULTS.....	18
VI. STATIC LOAD-CYCLE TEST SETUP.....	20
VII. SEISMIC LOAD SIMULATION AND ACCOMPANYING AIRFLOW.....	22
VIII. SUMMARY AND DISCUSSION.....	31
IX. RECOMMENDATIONS FOR FUTURE WORK.....	35
APPENDIX A. CONCRETE TEST CYLINDERS LAB REPORT.....	37
APPENDIX B. NEGATIVE WIND PRESSURE CALCULATION.....	43
B.1 SCOPE.....	44
B.2 BACKGROUND.....	44
B.3 STRATEGY.....	44
B.4 CALCULATION SUMMARY.....	45
B.5 CONCLUSION.....	46
REFERENCES.....	47

## FIGURES

1. CAP-1 test structure detail.....	8
2. CAP-1 test structure with cover plates attached.....	9
3. CAP-1 test structure forms and rebar before concrete placement.....	10

4	Permeability test setup.....	13
5.	Transient-pressure data for uncoated concrete shear wall permeability test.....	16
6.	Transient-pressure data for coated concrete shear wall permeability test.....	17
7.	Static load frame component layout.....	21
8.	Static test set.....	23
9.	CAP-1 load step vs load history.....	24
10.	CAP-1 60-psi NBSS load vs displacement curve, cycle 3.....	24
11.	CAP-1 130-psi NBSS load vs displacement curve, cycle 3.....	25
12.	CAP-1 190-psi NBSS load vs displacement curve, cycle 3.....	25
13.	CAP-1 285-psi NBSS failure load vs displacement cycle.....	27
14.	CAP-1 crack pattern on front (coated) side of shear wall.....	28
15.	CAP-1 crack pattern on back side of shear wall.....	29
16.	Typical transient-pressure decay plot after test structure damage.....	30
17.	Pressure variation over eight days during steady airflow test.....	32

## TABLES

I.	CONCRETE MIX CONSTITUENT PORTIONS.....	11
II.	MEASURED CONCRETE PROPERTIES.....	11
III.	CONCRETE SHEAR WALL PERMEABILITY.....	16
IV.	COATED CONCRETE SHEAR WALL PERMEABILITY.....	18
V.	COMPARISON OF PUBLISHED CONCRETE PERMEABILITIES.....	19

VI.	CONCRETE PERMEABILITY AFTER LINEAR SEISMIC LOAD- CYCLING RESPONSE.....	26
VII.	TRANSIENT PERMEABILITY DATA IN CRACKED CONCRETE SHEAR WALL.....	31
VIII.	STEADY PERMEABILITY DATA FOR CRACKED CONCRETE SHEAR WALL.....	32

# EXPERIMENTAL ASSESSMENT OF AIR PERMEABILITY IN A CONCRETE SHEAR WALL SUBJECTED TO SIMULATED SEISMIC LOADING

by

Steven P. Girrens and Charles R. Farrar

## ABSTRACT

A safety concern for the proposed Special Nuclear Materials Laboratory (SNML) facility at the Los Alamos National Laboratory was air leakage from the facility if it were to experience a design basis earthquake event. To address this concern, a study was initiated to estimate air leakage, driven by wind-generated pressure gradients, from a seismically damaged concrete structure. This report describes a prototype experiment developed and performed to measure the air permeability in a reinforced concrete shear wall, both before and after simulated seismic loading.

A shear wall (48 x 36 x 6 in.) test structure was fabricated with standard 4000-psi concrete mix. The percent of horizontal and vertical reinforcement in the shear wall was equal to the percent reinforcement proposed for the actual SNML structure. Static load-cycle testing was used to simulate earthquake loading. Permeability measurements were made by pressurizing one side of the shear wall above atmospheric conditions and recording the transient-pressure decay.

Air permeability measurements made on the shear wall before loading fell within the range of values for concrete permeability published in the literature. In addition, as long as the structure exhibited linear load-displacement response, no variation in the air permeability was detected. However, experimental results indicate that the air permeability in the shear wall increased by a factor of 40 after the wall had been damaged (cracked). Details of the experimental activities, comparisons of permeability data to published results, and recommendations for future work are presented.

## I. INTRODUCTION

Under normal operating conditions, the ventilation system for the proposed Special Nuclear Materials Laboratory (SNML) facility provides a negative pressure differential to prevent unfiltered air leakage from the building. Air leakage is the uncontrolled movement of air through walls and roofs both into a structure (infiltration) and out of a structure (exhaust). The air movement occurs as a result of pressure differences produced by wind, thermal effects, and the operation of mechanical ventilation systems. A loss of the ventilation system would allow the air pressure inside the building to equilibrate with the external ambient air pressure. Normal or extreme wind loading on the building will result in regions where the external stagnation pressure is up to 1 psi less than the internal pressure creating a driving potential for exhaust from the facility. A design basis earthquake (DBE) event could cause structural damage and ventilation system failure, thereby reducing the building's resistance to unfiltered exhaust. Estimating the exhaust rate from the SNML after a DBE event requires that the air permeability of the concrete walls, which have been loaded to their seismic-design limit, be quantified.

Because of its porous nature, concrete is known to be permeable to both liquids and gases. The objective of this study was to measure the air permeability of a reinforced concrete shear wall both before and after the wall had been loaded to its seismic-design limit. An experiment to satisfy this objective was developed by constructing a single-prototype shear wall test structure, simulating seismic loading by static load cycling the structure to its maximum-design shear stress, and performing air permeability tests on the structure both before and after loading. A shear wall structure was selected for initial study because this structural element forms a significant portion of the confining barrier and provides the dominant lateral load-carrying capability in the SNML facility. This report details the procedures used and results obtained during the course of the experiment.

## II. LITERATURE REVIEW

To obtain concrete with a consistency that allows it to be easily placed in forms and around rebar, more water than is necessary for the hydration of the cement is added to the mix. As the cement cures, excess water is trapped below the aggregate and between the cement particles. Most of these water voids are eliminated during the hydration of the cement. Initially, the hydration process produces a gel that forces most of the free water out of the mixture, but some water voids always remain. As the curing process continues, the gel solidifies and decreases in volume resulting in the formation of additional voids. Mixing of the concrete entraps air and further adds to the voids that are present. The water and air voids are typically interconnected causing the concrete to be permeable. Other leak paths will exist if the concrete cracks because of externally applied loads or because of adverse curing conditions. The use of air-entraining admixtures, typically specified for all structural concrete, should not affect the permeability of the concrete because the voids produced by these admixtures are not interconnected.

The flow rate of air through concrete depends upon the air permeability, the thickness of the concrete, and the pressure gradient applied. The air permeability coefficient is dependent upon the concrete mix parameters, mixing and compaction methods, curing conditions, and age. Typically, factors that improve the compressive strength of the concrete will decrease its permeability. Permeability increases with increasing water/cement (w/c) ratio. Curing reduces air permeability, but drying significantly increases permeability at any age. Although a specific concrete may be permeable to air, it may be impermeable to some other gases. Cracks and joints provide additional paths for air leakage. Air leakage rate through cracks is a function of the number of cracks, spacing, width, and penetration depth into the concrete. When cracks do not completely penetrate the concrete, the flow rate can be computed by assuming that the leakage is the air that flows through the uncracked concrete thickness.

The flow rate appears to be inversely proportional to the slab thickness and directly proportional to the pressure difference across the slab. Tests with pressure gradients up to 1.1 psi on concrete with

thicknesses varying from 4 in. to 9 in. give leakage rates in cubic inches per square foot per hour equal to approximately 2.5 times the ratio of pressure (psi) to thickness (in.).<sup>1</sup> These flow rates correspond to an air permeability coefficient through undamaged concrete of  $4.6 \times 10^{-6}$  in<sup>4</sup>/lb-s. This value for the permeability coefficient is typical for concrete with 4000-psi compressive strength at 28 days made with 3/4-in. maximum size aggregate, 500 lb cement per cubic yard, and a w/c ratio of 0.50.

A literature review covering the past 25 years examined published works on air permeability measurements in concrete. Most of the works reviewed dealt with gas flow and permeability measurements in undamaged concrete. In 1973, Figg<sup>2</sup> published a method for the *in situ* determination of the air permeability of concrete. The concept is based on (a) drilling a hole into the surface of the concrete, (b) sealing the top of the hole with a silicon rubber plug, (c) inserting a hypodermic needle through the plug, (d) drawing a vacuum in the hole, and (e) correlating any pressure increase in the hole with the air permeability in the concrete surrounding the hole. Despite being limited to a maximum of 1 bar in pressure differential, researchers found this method useful. Cather et al.<sup>3</sup> and Kasai et al.<sup>4</sup> modified the method for increased practicality. The 14.5-psi pressure limitation was overcome by Hansen et al.<sup>5</sup> who developed an apparatus that applies low air pressure to the surface and monitors the pressure increase over time in a hole drilled to a known depth under the pressurizing apparatus. All *in situ* procedures reviewed made air permeability measurements within 2 in. from the surface.

Several *in situ* and laboratory experiments were aimed at correlating air permeability with concrete characteristics. Kasai and coworkers<sup>6,7</sup> used their version of the *in situ* vacuum test apparatus to determine a relationship between air permeability and concrete carbonation. In addition, they determined that the air permeabilities of concrete with w/c ratios of 45% and 55% have about 1/4 the air permeability of concrete with a 65% w/c ratio. Laboratory experiments on concrete specimens of various dimensions were also used to characterize air permeability. Nagataki and Ujike<sup>8</sup> investigated the behavior of airflow through concrete containing fly ash and condensed silica. They found that the air tightness of concrete is improved with the addition of fly ash and silica fume because of these constituents' effect on porosity. Martialay<sup>9</sup> investigated the change in air

permeability of concrete slabs over a 20-year period and found that it stabilized in that period. Schonlin and Hilsdorf<sup>10</sup> confirmed the behavior of air permeability, which has been summarized previously, relative to curing, w/c ratio, and fly ash content. Laboratory tests to measure the intrinsic permeability of concrete were developed by Dhir et al.<sup>11</sup> As a result of this work, the air permeability test was found to provide a direct measure of the intrinsic permeability of concrete and results from the air test could be used to characterize hydraulic permeability.

A few research articles on airflow through penetrations and liner materials were also examined. The influence of air leakage through concrete is slight when compared with air leakage through construction joints. Tests were performed by Nojiri and Fujii<sup>12</sup> to investigate the air tightness of concrete with and without construction joints. Minimizing the air leakage through construction joints and penetrations was identified as a controlling efficiency factor if concrete was used for evaporator shells. The gas permeability characteristics of organic polymeric materials, suitable for use as liners in concrete containment structures, were studied experimentally by Epstein and coworkers.<sup>13</sup> The permeation of air, nitrogen, oxygen, krypton, and xenon was measured in polyvinyl chloride and chlorosulphonated polyethylene. This study concluded that, by using plastic liners, fission gas leak rates can be expected in the range of a few hundredths of a percent of the total contained volume per day.

The only study found in the literature dealing with airflow measurements in cracked reinforced concrete was published by Mayrhofer et al.<sup>14</sup> This study was aimed at determining the gas impermeability of shelter roof slabs loaded to their maximum carrying capacity with uniform pressure. The out-of-plane pressure load causes the slabs to bend. Gas impermeability for the slabs was defined by the ability to maintain a minimum overpressure of 0.5 to 1.0 mb. Square slabs with length dimensions of 45 in. and 118 in., 0.14% and 0.3% reinforcement by area, and a thickness of 7 in. were used in the experiments. The slabs were pressure loaded statically in monotonically increasing load steps. Airflow was measured upon completely unloading the structure after each load step. Data presented included static load-deformation curves, crack patterns, and airflow-overpressure curves. A mathematical expression to correlate slab

deflection with gas permeability was described in detail. A correlation between deformation and permeability was possible because the loading and resulting crack patterns in all slabs were similar.

In summary, the literature review indicated that the SNML study could use only the data published on gas permeabilities in undamaged concrete. These data were used to verify the accuracy of the air permeability measurements made on the test structure used in this investigation before applying any load. The experimental data reviewed, describing air permeability in cracked concrete, are not directly applicable because the structure tested was an out-of-plane, pressure-loaded slab. The initial SNML structure studied was a shear wall loaded in plane to its seismic-design shear stress limit.

### III. CONCRETE AIR PERMEABILITY, CAP-1, MODEL CONSTRUCTION

A reinforced concrete, shear wall test structure (CAP-1) was fabricated to support experiments to measure the air permeability in concrete after seismic loading. The CAP-1 test structure contains a 6-in.-thick shear wall that is a 3/7-scale model of an upper-level exterior wall for the proposed SNML facility.

The following construction information was supplied by the SNML Project Architect/Engineer, Fluor Daniel, and is representative of the Title I design. This information was incorporated into the design of the CAP-1 test structure.

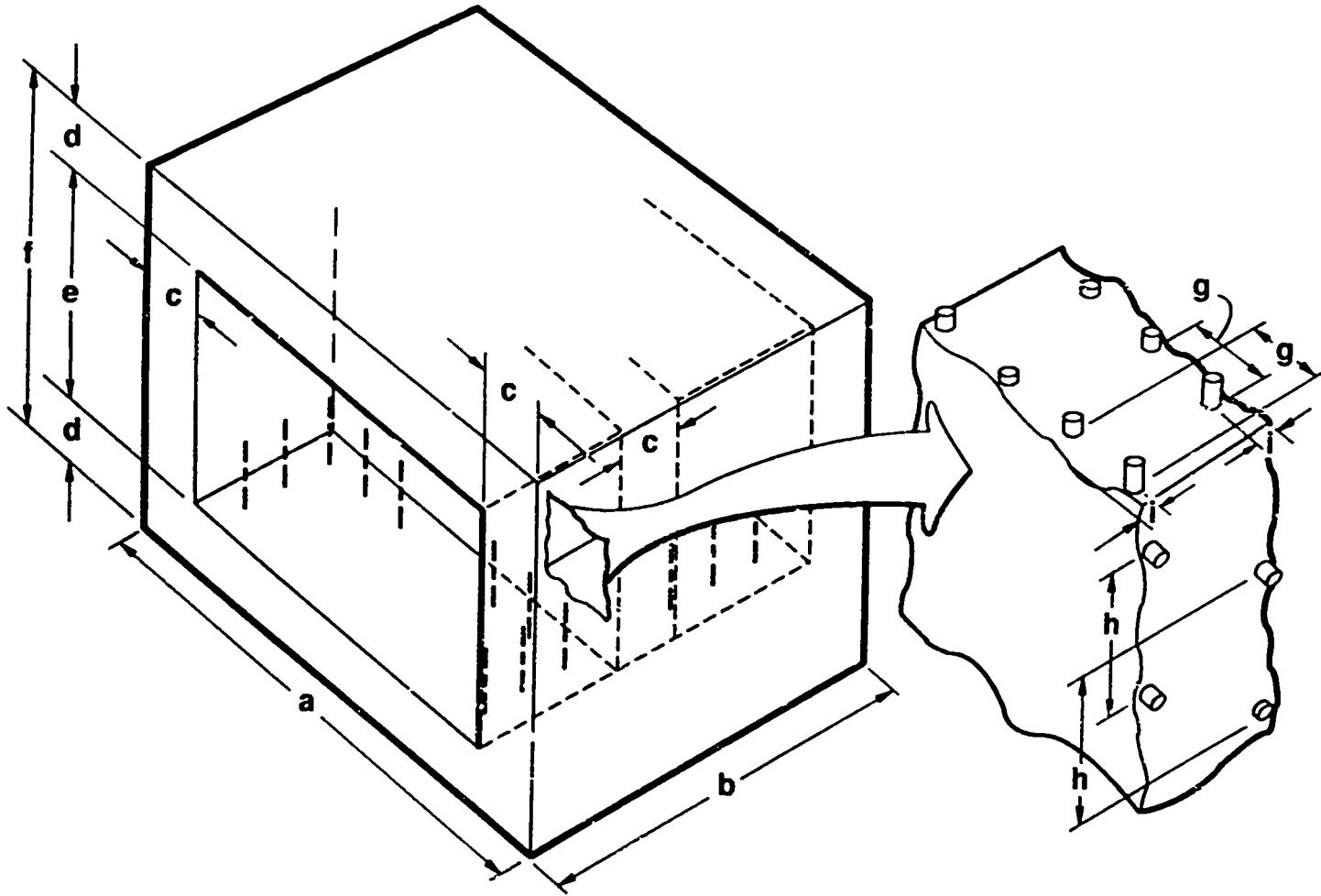
1. The concrete-design ultimate compressive strength is 4000 psi.
2. The minimum yield strength of the reinforcement is 60 000 psi (ASTM A615, Grade 60).
3. Typical wall reinforcement ratios, based on gross wall area, are 0.0113 vertical and 0.0037 horizontal.

4. The design concrete mix will incorporate conventional hardrock aggregate (approx. 1 in. maximum size), portland cement, and sand. Water-reducing agents will probably be used to achieve low-slump, low-w/c ratio and 4000-psi strength.

Figure 1 shows the dimensions of the CAP-1 model. Two layers of reinforcement (ASTM A615 Grade 60, No. 3 rebar, 0.375-in. diam) were placed throughout the model. Vertical layers were spaced at 3-in. centers providing a 1.15% wall reinforcement ratio by area. Horizontal layers were spaced at 6-in. centers providing a 0.41% wall reinforcement ratio by area. Hook development lengths and minimum bend radii for the reinforcement were specified to meet the requirements of ACI 318-83 (Ref. 15) sections 12.5 and 7.5, respectively. A minimum of 1.0 in. of cover was provided for all reinforcement.

The structure was formed with Plexiglas so that the surfaces could be visually monitored during the concrete placement and compaction. Aluminum spacer rods were used to maintain proper clearances between the rebar and the forms during the concrete placement. Six conduits (0.825-in. i.d.), extending completely through the top of the model from end wall to end wall, were placed in the top slab. The conduits accommodated 0.75-in. threaded rods that were used to attach bearing plates during static loading. Twenty 0.5-in. threaded rods were located every 6 in. along the center of the concrete face bordering each open end of the test structure. These rods were used to attach the aluminum cover plates as shown in Fig. 2. Twenty 1.25-in. bolts were placed through sleeves in the base to restrain the structure during the static load cycling. Figure 1 shows the bolt pattern on one side of the shear wall. Figure 3 shows the forms and reinforcement before placement of the concrete.

The concrete for CAP-1 was placed on July 31, 1990. CAP-1 was placed from 2 cubic yards of concrete from a commercial source that arrived at 12:45 p.m. The concrete mix was specified to have 4000-psi nominal ultimate compressive strength, a 4.0-in. slump, and a 0.75-in. maximum aggregate size. Table I summarizes the mix portions. The slump was measured per ASTM C143 (Ref. 16) and was found to be 3.5 in. The w/c ratio of the concrete was 0.35. Concrete was placed in the base of



STRUCTURE	DIMENSIONS (in.)									REBAR diam	MAX AGGREGATE SIZE
	a	b	c	d	e	f	g	h	i		
MODEL 1	48	36	6	6	24	36	3	6	1	0.375	0.75

Fig. 1. CAP-1 test structure detail.

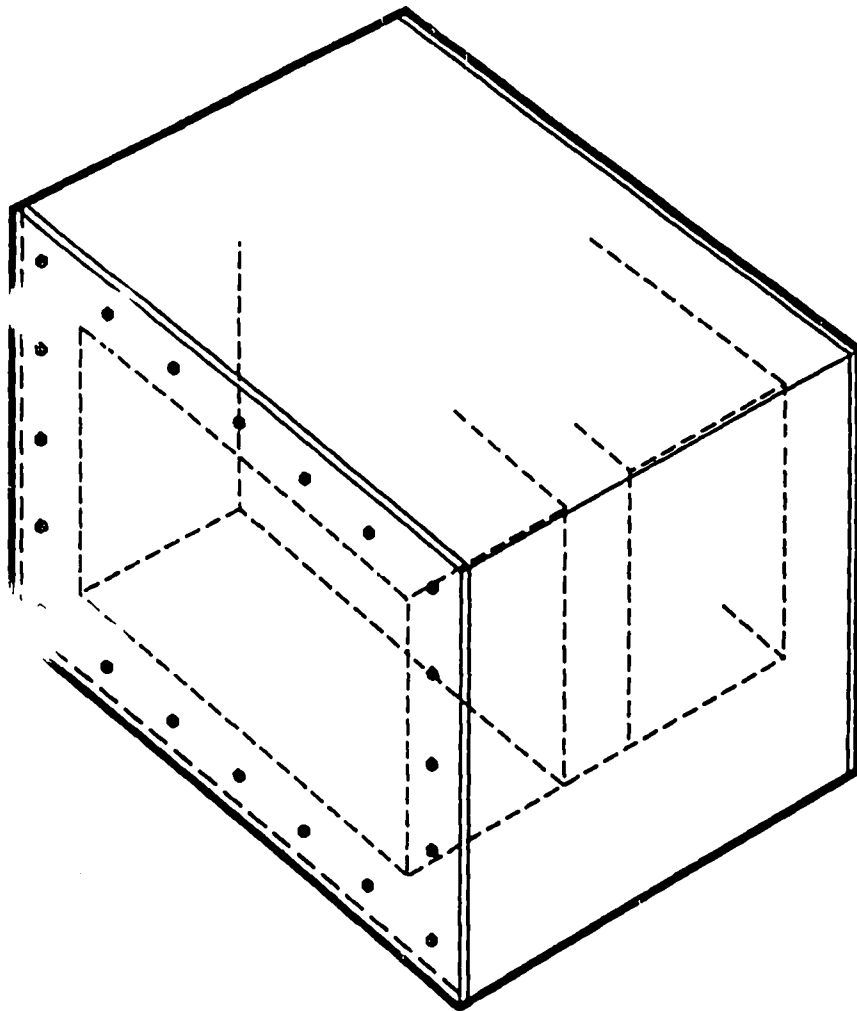


Fig. 2. CAP-1 test structure with cover plates attached.

the structure first and was compacted with mechanical vibrators. Next, the walls were placed and compacted with mechanical vibrators as the aluminum spacer bars were removed. CAP-1 was completely placed by 1:30 p.m. No defects were noticed on the surface of the structure after the compaction was complete. The structure was left in its form for a 28-day curing period, and exposed surfaces were kept moist and covered with a tarp.

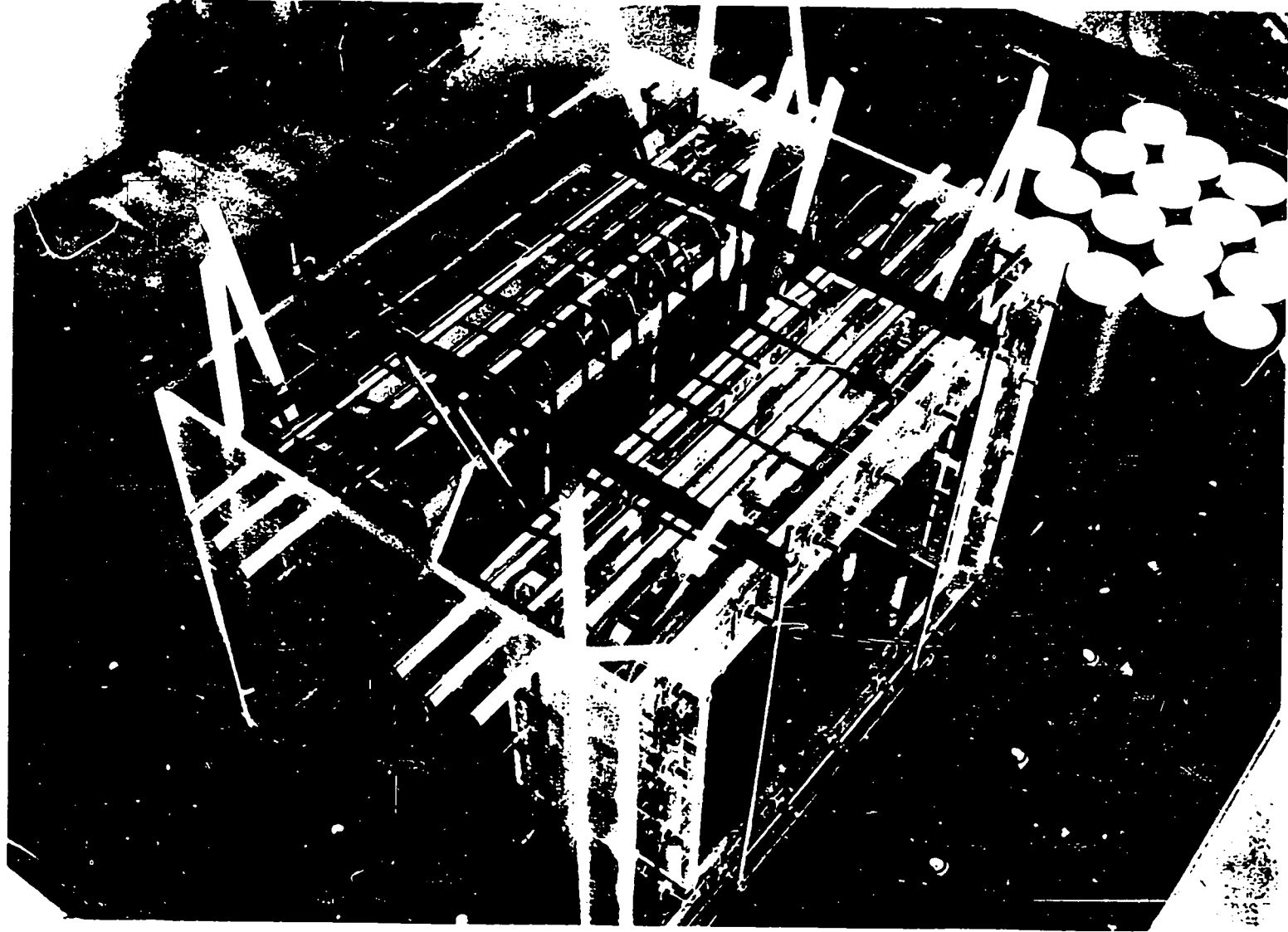


Fig. 3. CAP-1 test structure forms and rebar before concrete placement.

During the placement of the structure, fifteen standard 6-in.-diam by 12-in.-high test cylinders were taken per ASTM C172 (Ref. 18) and ASTM C31 (Ref. 18). The test cylinders were left in their mold and cured with the structure for 28 days. Tests on the cylinders included ultimate compressive strength (ASTM C39),<sup>19</sup> modulus of elasticity (ASTM C469),<sup>20</sup> and split-cylinder tensile strength (ASTM C496).<sup>21</sup> The cylinders were tested on October 2, 1990, by Western Technologies in Albuquerque. From the group of fifteen cylinders, ten were tested for ultimate strength and modulus and five were tested for split-cylinder tensile strength. The results of the concrete tests are summarized in Table II, and the report from the testing lab is included as Appendix A.

TABLE I  
CONCRETE MIX CONSTITUENT PORTIONS

<u>Constituent</u>	<u>Weight (lb)</u>
Sand	3030
Coarse aggregate	3420
Cement	1232
Water	434

TABLE II  
MEASURED CONCRETE PROPERTIES

	<u>Ultimate Compressive Strength (psi)</u>	<u>Tensile Strength (psi)</u>	<u>Modulus of Elasticity (psi)</u>
Average	6086	516	$4.62 \times 10^6$
Minimum	5720	440	$4.11 \times 10^6$
Maximum	6670	600	$4.87 \times 10^6$

#### IV. AIR PERMEABILITY TESTING

Air permeability measurements were made on the shear wall before exposing the test structure to static load cycling. The air permeability was determined by pressurizing one side of the test structure slightly above atmospheric levels and recording the transient-pressure decay associated with the air leakage through the shear wall.

To accommodate structure pressurization, an aluminum cover plate (40 x 52 x 3/4 in.) was attached to the structure as shown in Fig. 2. The cover plates provided resistance and sealing support for internal pressurization. Square (0.275-in.) BUNA-N O-ring cord stock and Abeazon vacuum sealant were used to form a seal between the concrete face and the cover plate. In later permeability tests, flooring contact cement was also used to ensure an airtight seal between the O-ring material and the concrete face. The interior surfaces of the side walls and the top and bottom slabs on the side of the shear wall to be pressurized were spray painted with three coats of epoxy paint to ensure impermeability. Internal pressurization of the test structure did not exceed 0.7 psig. The pressurized volume, 7.5 cu ft, was filled with dry bottled air and purged with a vacuum pump three times before filling for test. Pressure levels were monitored with a Paroscientific digiquartz pressure transducer having a range of 0 to 30 psia and a resolution of 0.0001 psia. After pressurization, transient internal pressure, atmospheric pressure, and internal temperature were monitored with a Hewlett Packard 3497A data scanner. Figure 4 shows the permeability test setup.

In these experiments the permeability coefficient that was determined is referred to in the literature as the intrinsic permeability. The intrinsic permeability is dependent only on the internal structure of the concrete and is independent of the properties of the migrating fluid. Air permeability tests best characterize the intrinsic permeability of concrete. For the direct measurement of the permeability of concrete in accordance with Darcy's law, conditions of steady-state flow should exist. The intrinsic permeability can be expressed by the following relation:

$$Q/A = - k/\mu(dp/dl) \quad , \quad (1)$$

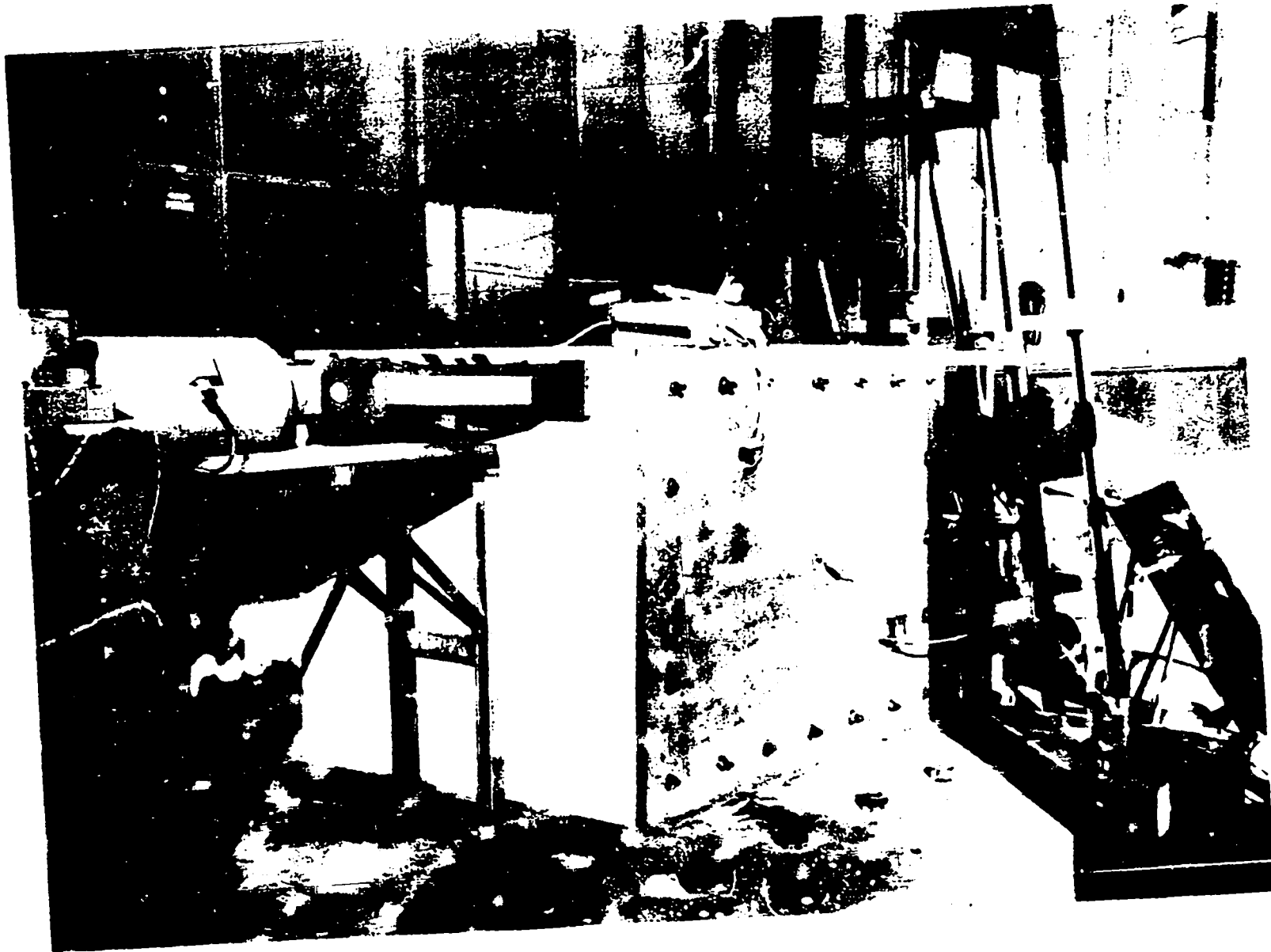


Fig. 4. Permeability test: setup.

where  $Q$  is the volume rate of flow,  $A$  is the cross-sectional area perpendicular to the flow direction,  $k$  is the intrinsic permeability,  $\mu$  is the dynamic viscosity, and  $dp/dx$  is the pressure gradient in the direction of flow. For a compressible gas, the volume flow rate varies with change of pressure according to the relationship

$$P_m Q_m = \text{constant} = PQ \quad (2)$$

where

$$P_m = \sqrt{\frac{1}{2}(P_t + P_{t+\Delta t})}$$

$P_t$  and  $P_{t+\Delta t}$  correspond to readings of the pressurized volume at times  $t$  and  $t+\Delta t$ , respectively, and  $Q_m$  is the flow rate at the mean pressure,  $P_m$ . Upon substituting the relationship for  $Q$  shown in Eq. (2) into Eq. (1) and noting that the outlet pressure will be atmospheric, the direct integration of Eq. (1) can be performed over the wall thickness and corresponding inlet and outlet pressures to obtain

$$k = 2\mu L P_m Q_m / \Lambda (P_m^2 - P_{ATM}^2) \quad (3)$$

where  $P_{ATM}$  is the atmospheric pressure and  $L$  is the length of the concrete in the flow direction. The volume flow rate passing through the shear wall can be expressed as

$$Q = \Delta m / \rho \Delta t \quad (4)$$

where  $\rho$  is the density and  $\Delta m$  is the incremental change in the mass during the time increment  $\Delta t$ . Assuming that the airflow behaves in accordance with the ideal gas law, the incremental mass can be expressed as

$$\Delta m = V(P_t/T_t - P_{t+\Delta t}/T_{t+\Delta t})/R \quad (5)$$

where  $R$  is the ideal gas constant,  $V$  is the volume that is pressurized, and  $T$  corresponds to absolute temperature. Substituting Eq. (5) into Eq. (4) and noting that  $\rho_m = P_m/RT_m$  yields

$$Q_m = T_m V (P_t/T_t - P_{t+\Delta t}/T_{t+\Delta t}) / P_m \Delta t \quad (6)$$

Substituting Eq. (6) into Eq. (3), the permeability coefficient in the shear wall is calculated with the expression

$$k = 2\mu L V T_m (P_t/T_t - P_{t+\Delta t}/T_{t+\Delta t}) / A \Delta t (P_m^2 - P_{ATM}^2) \quad (7)$$

The following values and units were used in Eq. (7):

$$\begin{aligned} k &= [\text{in}^2], \\ \mu &= [\text{lb-s/ft}^2], \\ L &= 0.5 \text{ ft}, \\ V &= 7.5 \text{ ft}^3, \\ A &= 6.0 \text{ ft}^2, \\ t &= [\text{s}], \\ P &= [\text{psi}], \text{ and} \\ T &= [R]. \end{aligned}$$

Transient pressure and temperature data were recorded over a period of seven days. These data are shown in Fig. 5. The volume was initially pressurized to approximately 12 psia. After three days of data collection, the volume was again repressurized. The actual data used to compute  $k$ , using Eq. (7), were the specific values recorded at midnight on each day. This was done to average out the wide variation in temperature because the experiment was located outside. Table III lists the recorded pressures and temperatures along with the computed air permeabilities.

In the above calculations for permeability, the dynamic viscosity of air was assumed to vary with temperature according to the relation

$$\mu = (5.672 \times 10^{-5} T + 0.0338) \times 10^{-5} \text{ lb-s/ft}^2 ,$$

where  $T$  is in degrees F.

TABLE III  
CONCRETE SHEAR WALL PERMEABILITY

$P_1$ (psi)	$T_1$ (R)	$P_{1+\Delta t}$ (psi)	$T_{1+\Delta t}$ (R)	$P_{ATM}$ (psi)	$k$ ( $\times 10^{-13}$ in <sup>2</sup> )
11.9467	519.5	11.8451	522.5	11.3032	0.414
11.9134	522.5	11.8074	523.5	11.3194	0.451
11.8306	523.5	11.7151	523.1	11.2844	0.521
11.9567	521.1	11.8027	516.1	11.3586	0.637
11.6875	516.2	11.6043	516.3	11.2384	0.404
11.6071	516.3	11.5066	518.2	11.2298	0.918

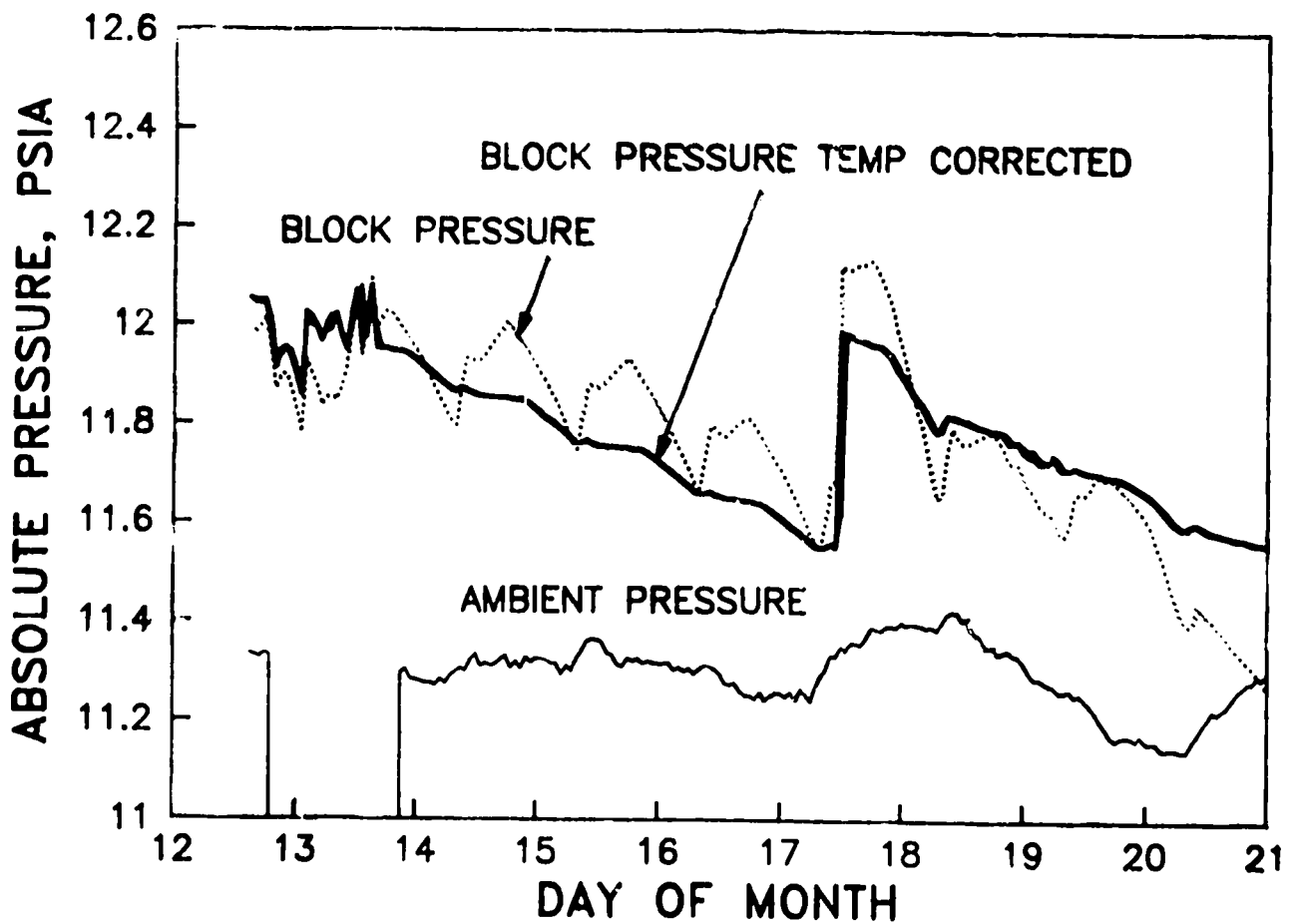


Fig. 5. Transient-pressure data for uncoated concrete shear wall permeability test.

After the first series of permeability tests were performed on the shear wall structure, the concrete was coated with a decontaminable coating system. The special coating system was applied in four distinct layers: (1) an epoxy clear sealer, (2) a chemical-resistant patching compound, (3) a strike flush coat of surfacing enamel, and (4) a spray-applied body coat of surfacing enamel. The primary purpose of the coating system is to permit the efficient decontamination of concrete walls and ceilings. In this experiment, the coating system was applied to measure its affect on concrete permeability.

After the coating system was allowed to cure, transient pressure and temperature data were recorded over a period of three days. The data are illustrated graphically in Fig. 6. Twenty-four-hour data used to compute the concrete permeability are listed in Table IV. The coating

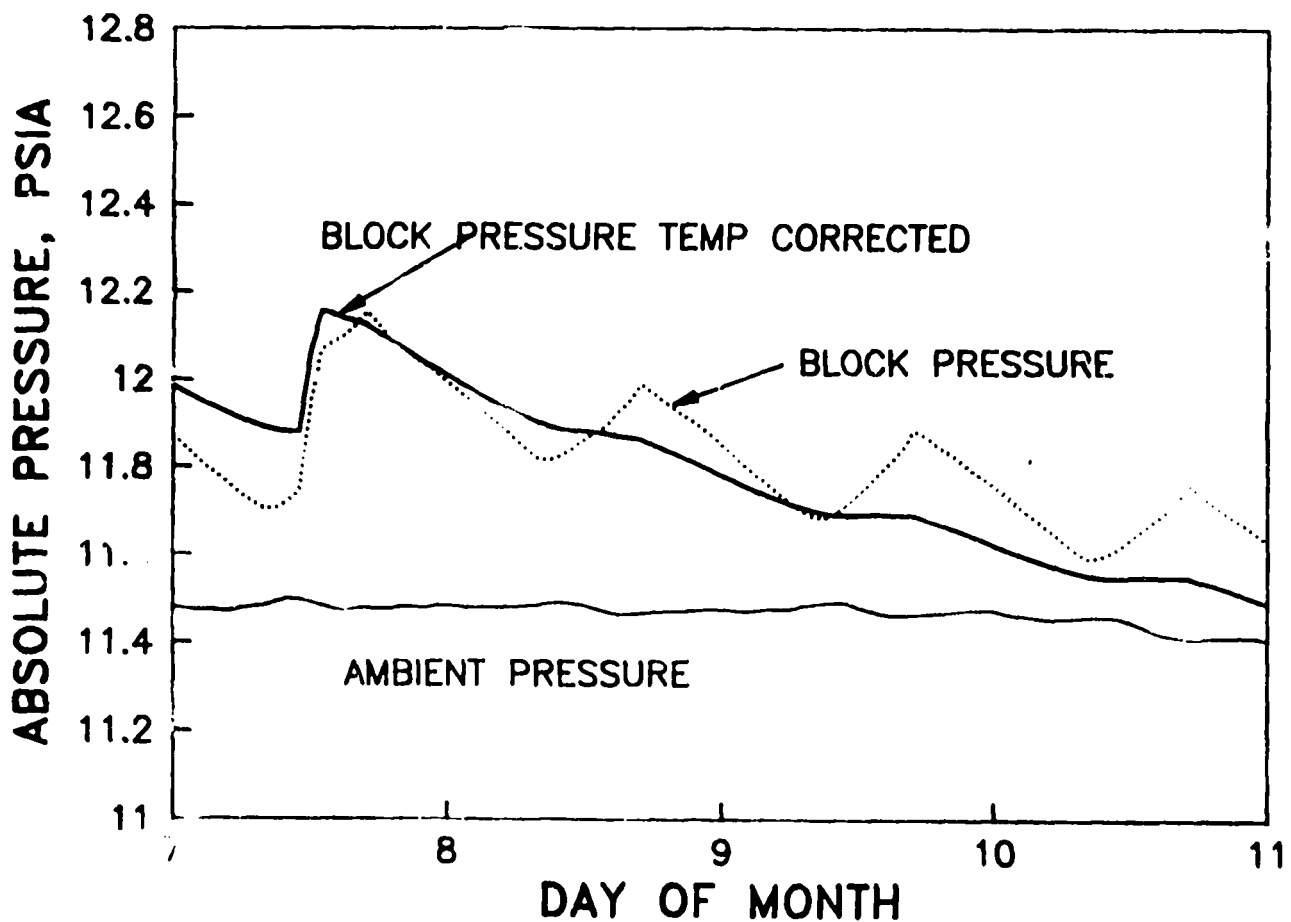


Fig. 6. Transient-pressure data for coated concrete shear wall permeability test.

TABLE IV  
COATED CONCRETE SHEAR WALL PERMEABILITY

$P_i$ (psi)	$T_i$ (R)	$P_{i+\Delta t}$ (psi)	$T_{i+\Delta t}$ (R)	$P_{ATM}$ (psi)	$k$ ( $\times 10^{-13} \text{ in}^2$ )
11.9943	491.7	11.7789	491.8	11.4808	1.27
11.8509	491.7	11.7033	491.8	11.4760	1.18
11.7584	491.8	11.6323	491.8	11.4443	1.22

system had no impact on the measured concrete permeability because, as evident when comparing Tables III and IV, the permeability increased. The increase in permeability was most likely caused by the additional seven weeks of concrete drying time because drying significantly increases the permeability.<sup>1,11</sup>

#### V. COMPARISON OF PERMEABILITY DATA WITH PUBLISHED RESULTS

In this section, the measurement of air permeability in concrete by others will be summarized. The experiments described were all performed in laboratory settings on small concrete samples.

Measurements of the intrinsic permeability of concrete were performed by Dhir et al.<sup>11</sup> using an air permeability test. Pressure cells were designed to test 100-mm- and 50-mm-diameter by 50-mm-thick test specimens that were subjected to an externally maintained constant air pressure at one end and atmospheric pressure at the other and while the circumferential surface was sealed. The air supply to the cell was dried to less than 0.1% RH. Before testing, specimens were conditioned using 105°C oven drying. After conditioning, the test specimen was placed in the pressure cell and an inlet pressure of 0.34 MPa was applied. When the measured inlet and outlet flow rates equilibrated, the steady-state flow rate and inlet pressure were recorded. Permeability data were presented for various specimen-curing and w/c ratios. Table V summarizes the data published for concrete specimens cured for 28 days in air at 20°C with 55% RH.

TABLE V  
COMPARISON OF PUBLISHED CONCRETE PERMEABILITIES

Reference	w/c	Compressive Strength (psi)	k (x 10 <sup>-13</sup> in <sup>2</sup> )
11	0.4	9425	2.4
11	0.47	7975	4.0
5	0.4	12500	0.08
5	0.55	3770	0.66
8	0.4	-	0.4-1.0
8	0.3	-	0.6
22	0.56	6815	0.13-5.3

Hansen et al.<sup>5</sup> described a method, theory, and portable apparatus for estimating the gas permeability of concrete *in situ*. The test applies low air pressure to the surface of the concrete and monitors the pressure increase, over time, for a given depth, as a measure of the air permeability. Three sets of 200-mm cubes were prepared for three different w/c ratios, 1.00, 0.55, and 0.40. A specially designed drill jig is used to cut a hole to a predetermined depth below the surface. A pressure head is attached on the concrete surface directly above the end of the drilled hole. Pressure sensors are used to detect pressure changes in the concrete below the pressure head. Pressures around 150 kPa are applied to the surface and the rate of pressure increase in the hole, over time, is recorded. The air permeability is obtained by comparing the pressure-time curves experimentally measured to solutions of the 1-D conservation of mass equation incorporating Darcy's law. Air permeabilities that were determined, using this procedure, are contained in Table V.

Nagataki and Ujike confirmed that the flow of air through concrete obeyed Darcy's law.<sup>8</sup> Concrete prisms 150 mm by 150 mm and 530 mm in length were cast for various w/c ratios. After water curing for 28 days, the specimens were conditioned in air at 20°C and 60% RH until tested. Test specimens were cut to 120 mm in length, and the four sides parallel to the airflow direction were coated with epoxy resin. The specimens were set in a pressure vessel, and one side was subjected to pressures in the range 0.2 to 0.6 MPa. The quantity of airflow through the concrete was

measured after the flow reached steady state. The air permeability of the concrete specimens was found to increase with the increase of w/c ratio and the length of drying period. Air permeabilities reported in this publication are listed in Table V.

Huovinen<sup>22</sup> measured the volume flow rate of air through cylindrical concrete specimens 150 mm in diameter and 60 to 100 mm in thickness. The specimens were also tested in steel pressure cells. The space between the specimen and steel cell was made airtight by filling the void with bitumen. Compressed air was applied to one side of the specimen with pressures in the range 1 bar to 5 bar. The measured range of steady-state air permeabilities reported in this research is also listed in Table V.

The *Handbook of Concrete Engineering*<sup>1</sup> infers that an air permeability of  $0.12 \times 10^{-13}$  in<sup>2</sup> is typical for concrete with 4000-psi compressive strength and a w/c ratio of 0.5. As can be seen in Table V, the permeability of air in concrete varies by more than an order of magnitude above this value even among well-controlled experiments in the laboratory. The "as constructed" air permeabilities measured in this experiment ( $1.2 \times 10^{-13}$  in<sup>2</sup>) are well within the range of published values. In addition, the measurements taken during this experiment were not obtained from laboratory specimens but from an actual shear wall structure that was cured in the field.

## VI. STATIC LOAD-CYCLE TEST SETUP

The model was constructed in place on the load frame base that was to be used in the cyclic testing. The load frame base consisted of two 90 x 120 x 6 in. steel plates bolted together with 1.25-in. steel bolts. The test structure was attached to the load frame with twenty 1.25-in. bolts and 3.5 x 4 x 0.25 in. washers as shown in Fig. 1. The bolts were torqued to 250 ft-lb.

The steel load frame was assembled adjacent the test structure. A layout of the major load frame components is shown in Fig. 7. An instrumentation frame was located on the exterior side of the model opposite the load frame. Two Ono-Sokki EG-233 displacement transducers



were placed against the model 3 in. from the top and bottom of the test structure and centered in the midplane of the shear wall. These transducers were used to measure overall structural deformation. An ENERPAC hydraulic actuator was used to load the structure, and force input was monitored with a Transducers Model T42 load cell located between the actuator and the steel load-distribution yoke. At specified load increments, the displacement transducers and load cell were scanned with a Hewlett Packard 3497A data scanner and the results were recorded by a Hewlett Packard 87 computer. Figure 8 shows the static test setup.

The structure was loaded for 3 cycles each to nominal base shear stress (NBSS) levels of  $\pm 60$  psi,  $\pm 130$  psi, and  $\pm 190$  psi. In this context, NBSS is defined as the applied force divided by the cross-sectional area of the shear wall (288 in<sup>2</sup>). During each cycle, readings from the load cell and displacement transducers were made at increments of 1/5 the peak load. The actual load history is shown in Fig. 9. Each integer on the horizontal axis in Fig. 9 represents a point at which the data were scanned. Load-displacement plots were prepared for each cycle of loading. The complete load reversals shown in the load history were applied to represent the force induced in a structure during seismic excitation. These quasi-static load cycles simulate an earthquake by applying the positive and negative shear forces associated with a DBE to the structure. This loading procedure was recommended for use by the Technical Review Group evaluating the United States Nuclear Regulatory Commission sponsored Seismic Category I (SCI) Structures Program at Los Alamos.<sup>23-25</sup>

## VII. SEISMIC LOAD SIMULATION AND ACCOMPANYING AIRFLOW

The overall horizontal deformation versus load curves were constructed from the displacement transducer and load cell measurements and are shown in Figs. 10-12. The displacements represent a total displacement for the top measurement location relative to the bottom measurement location. Only the third load cycle for each set of 60-, 130-, and 190-psi NBSS are shown. The structure showed linear response through all of the load cycles. This indicated that the structure experienced no internal damage when loaded up to the maximum nominal-design shear

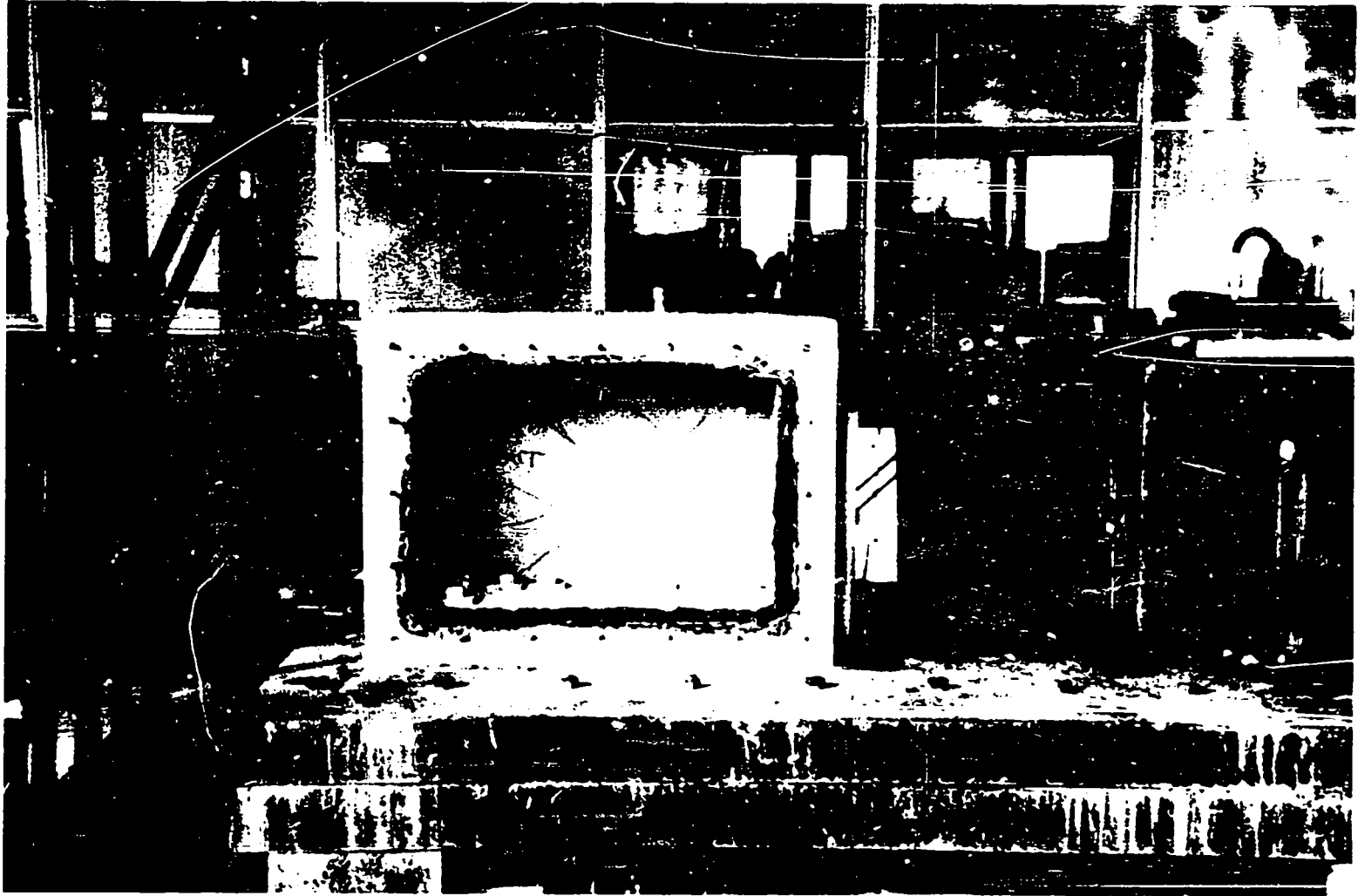


Fig. 8. Static test setup.

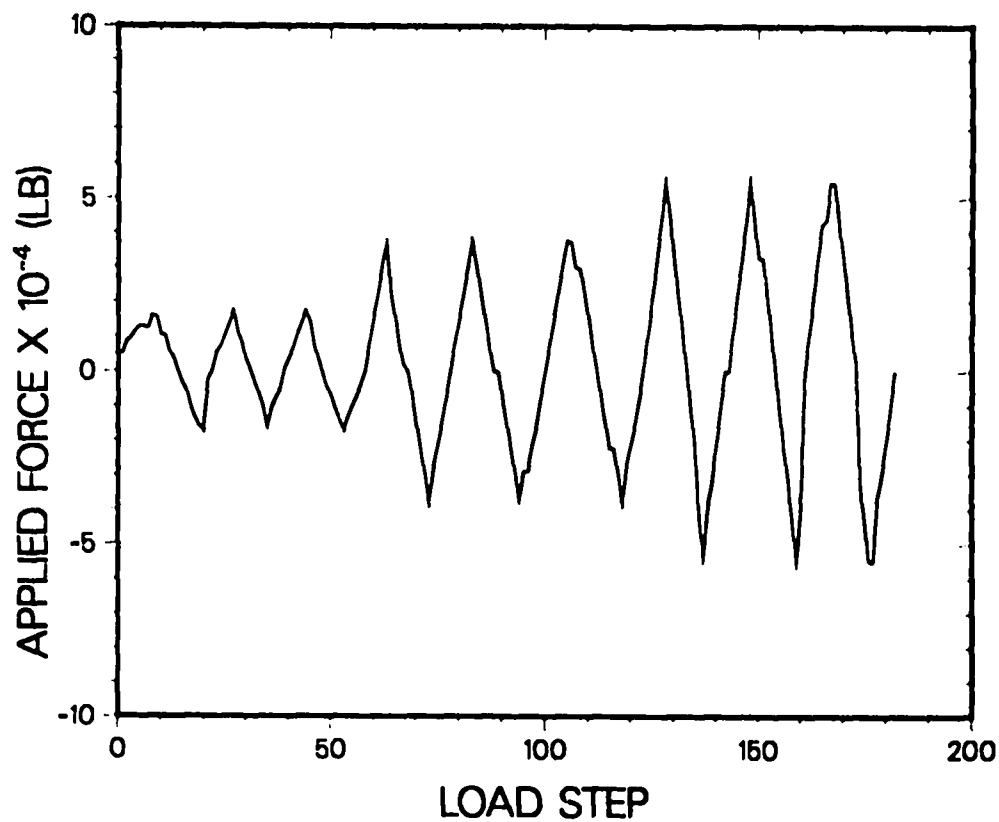


Fig. 9. CAP-1 load step vs load history.

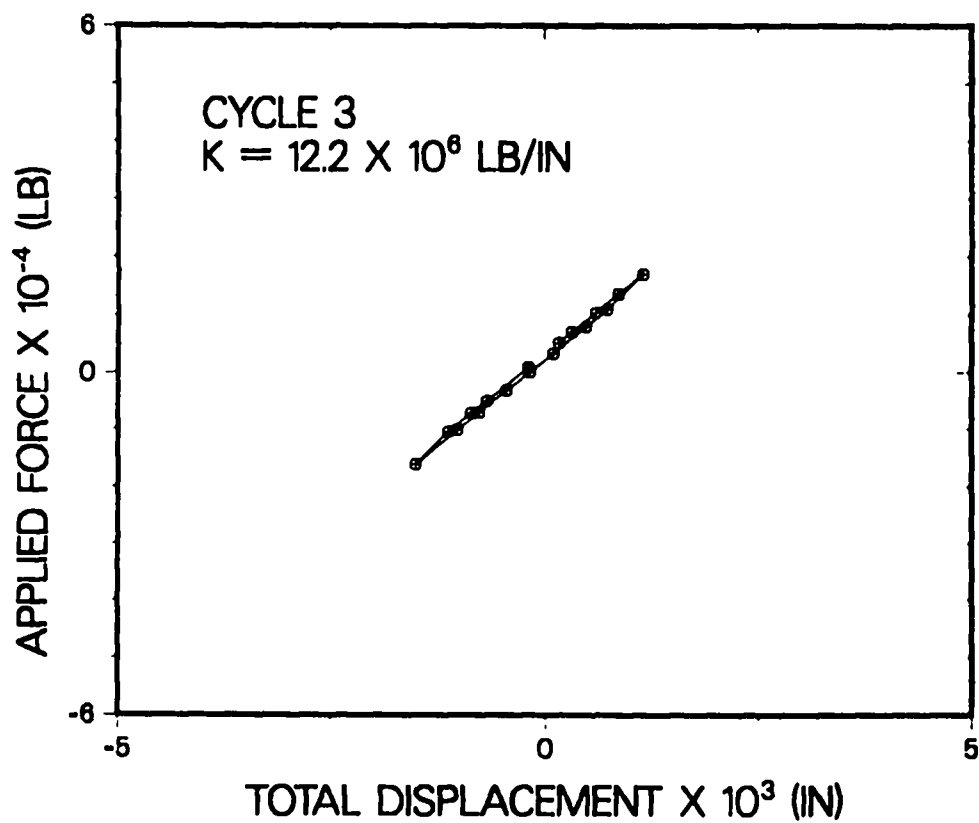


Fig. 10. CAP-1 60-psi NBSS load vs displacement, cycle 3.

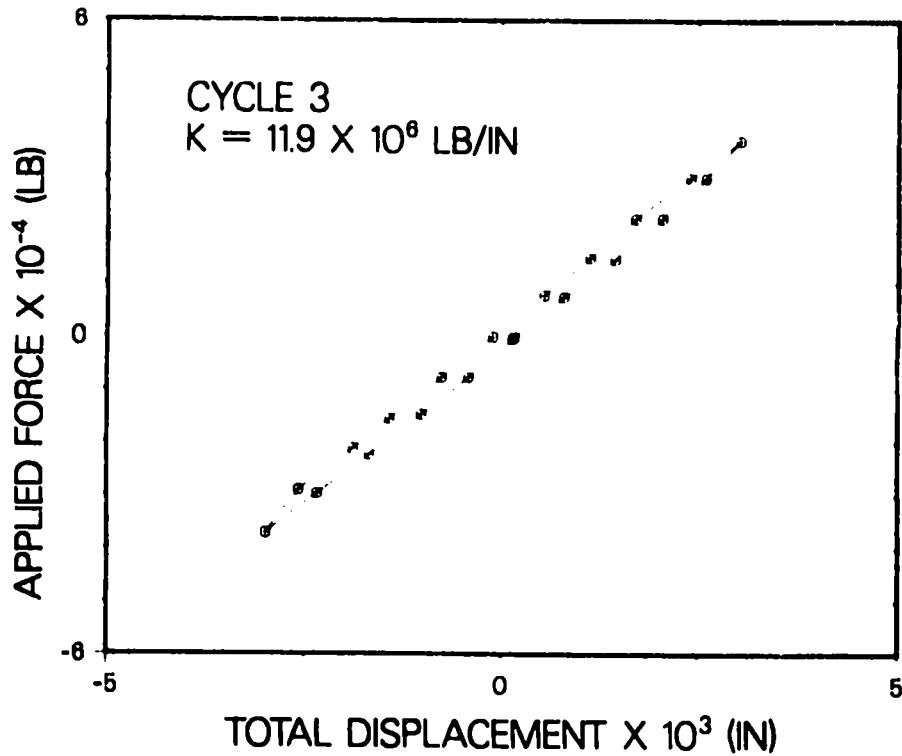


Fig. 11. CAP-1 130-psi NBSS load vs displacement, cycle 3.

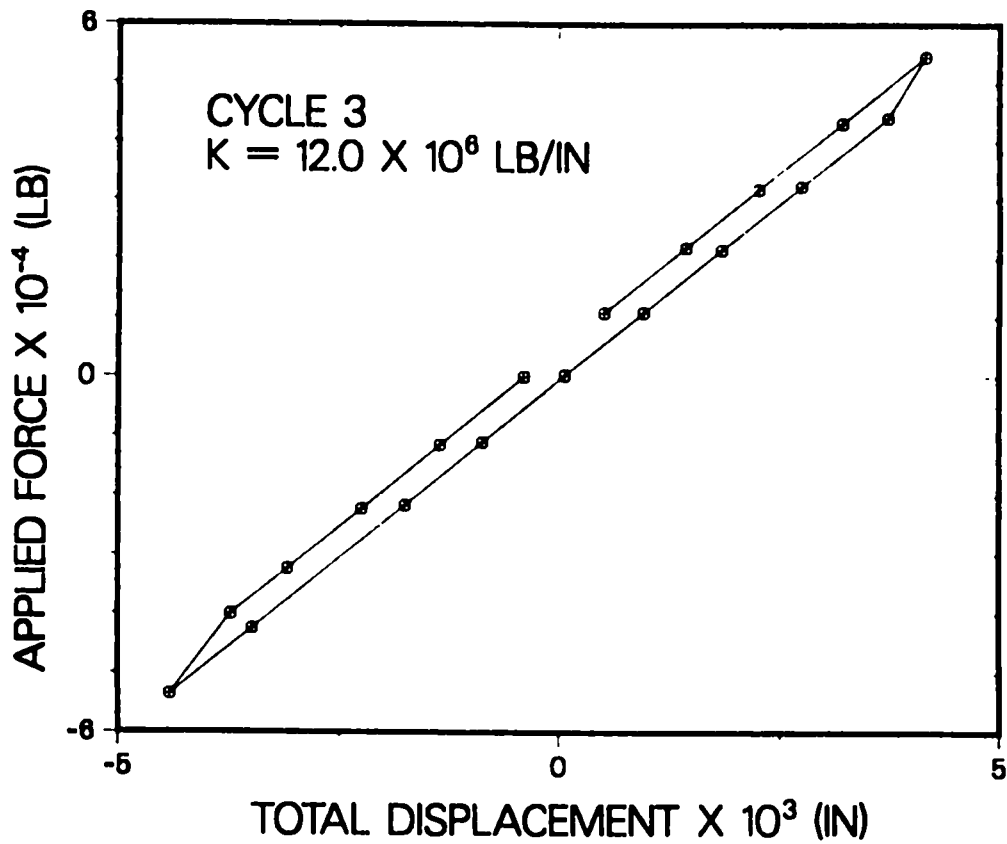


Fig. 12. CAP-1 190-psi NBSS load vs displacement, cycle 3.

stress of 190 psi. Stiffnesses calculated using the load-displacement data are within 7% of the structural stiffness determined from a 3-D finite element analysis (FEA) of the test structure. The variation is most probably caused by the fact that the base boundary condition in the FEA assumes an ideal fixed condition, whereas the base of the test structure is bolted to the load frame. The test cylinder data only provide an estimate of the actual concrete material properties. The test cylinder data were used in the FEA, and the actual properties of the structure could be different from those obtained from these data.

Because the structure experienced no internal damage, the concrete air permeability was also not affected. This is evidenced by the three days of pressure data contained in Table VI. The air permeabilities computed with these data are in agreement with the preload data listed in Table IV.

Next, the structure was subjected to one 285-psi NBSS load cycle. The SNML Project Architect/Engineer, Fluor Daniel, requested that the test structure be loaded to an NBSS level 50% above the seismic-design level of 190 psi. Figure 13 shows the load-displacement curve constructed from the data taken during the single high-level load cycle. The structure cracked on the first load increment above the 190-psi NBSS level. Confirmation that cracking occurred is evident from the change in slope of the load-displacement curve in the positive direction. The load-displacement curve also indicated cracking through stiffness reduction during loading in the negative direction of the cycle. Actual shear wall

TABLE VI  
CONCRETE PERMEABILITY AFTER  
LINEAR SEISMIC LOAD-CYCLING RESPONSE

$P_1$ (psi)	$T_1$ (R)	$P_{1+\Delta t}$ (psi)	$T_{1+\Delta t}$ (R)	$P_{ATM}$ (psi)	$k$ ( $\times 10^{-13}$ in <sup>2</sup> )
11.9866	491.8	11.7505	491.7	11.3664	1.14
11.7060	491.6	11.5848	491.7	11.3612	1.05
11.4631	491.7	11.3920	491.7	11.2880	1.26

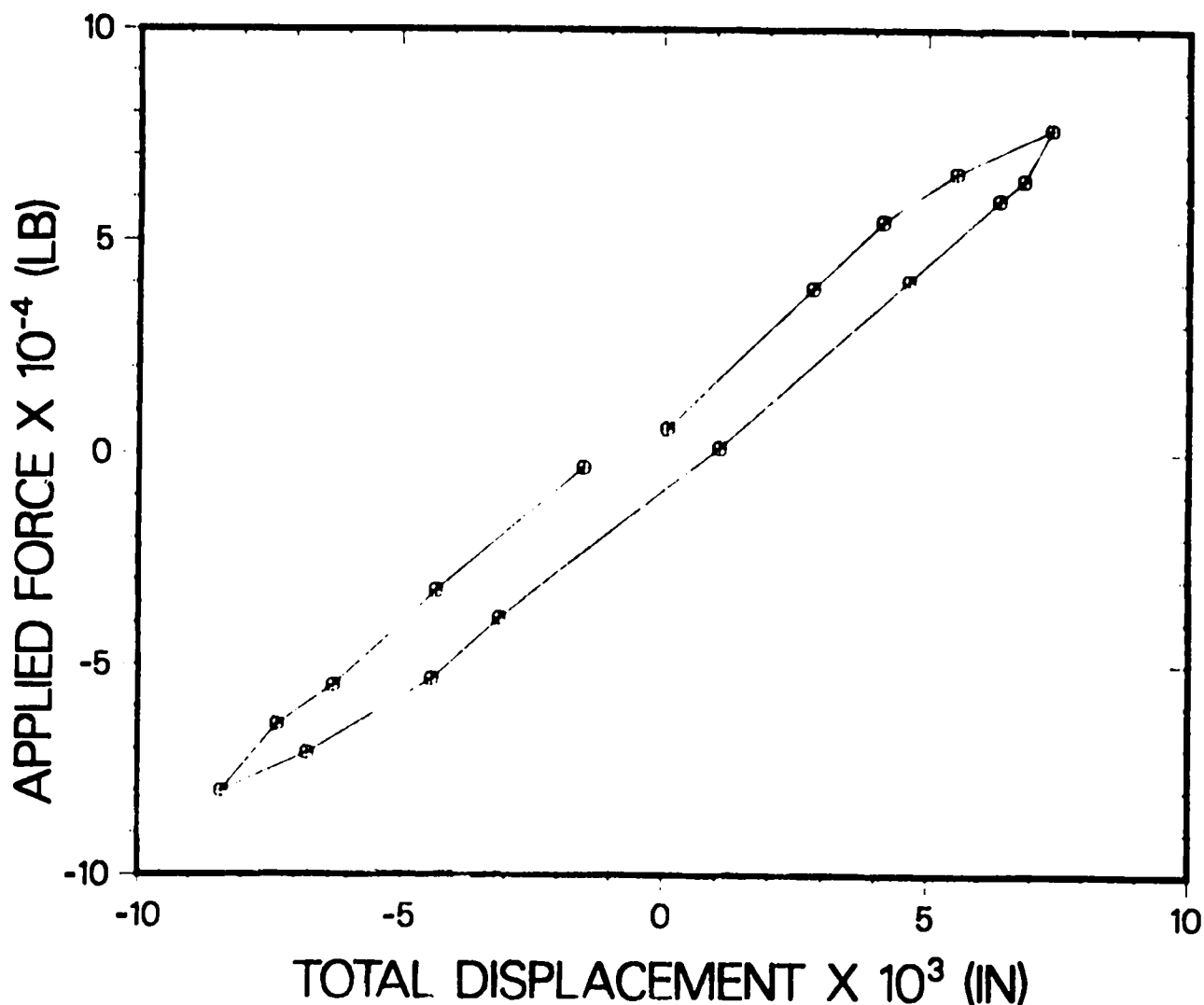


Fig. 13. CAP-1 285-psi NBSS failure load vs displacement cycle.

crack patterns are shown in Figs. 14 and 15. Most of the shear cracks identified penetrated completely through the wall. The positive and negative direction cracking loads of 60 670 lb (211-psi NBSS) and 62 760 lb (218-psi NBSS), respectively, were determined by computing the load at the intersection of the load-displacement curves corresponding to the uncracked and cracked structural response. Based on a comparison with data taken during the SCI Program tests,<sup>23-25</sup> this test structure was predicted to crack at 230-psi NBSS when its average measured tensile strength of 516 psi was considered.



Fig. 14. CAP-1 crack pattern on front (coated) side of shear wall.

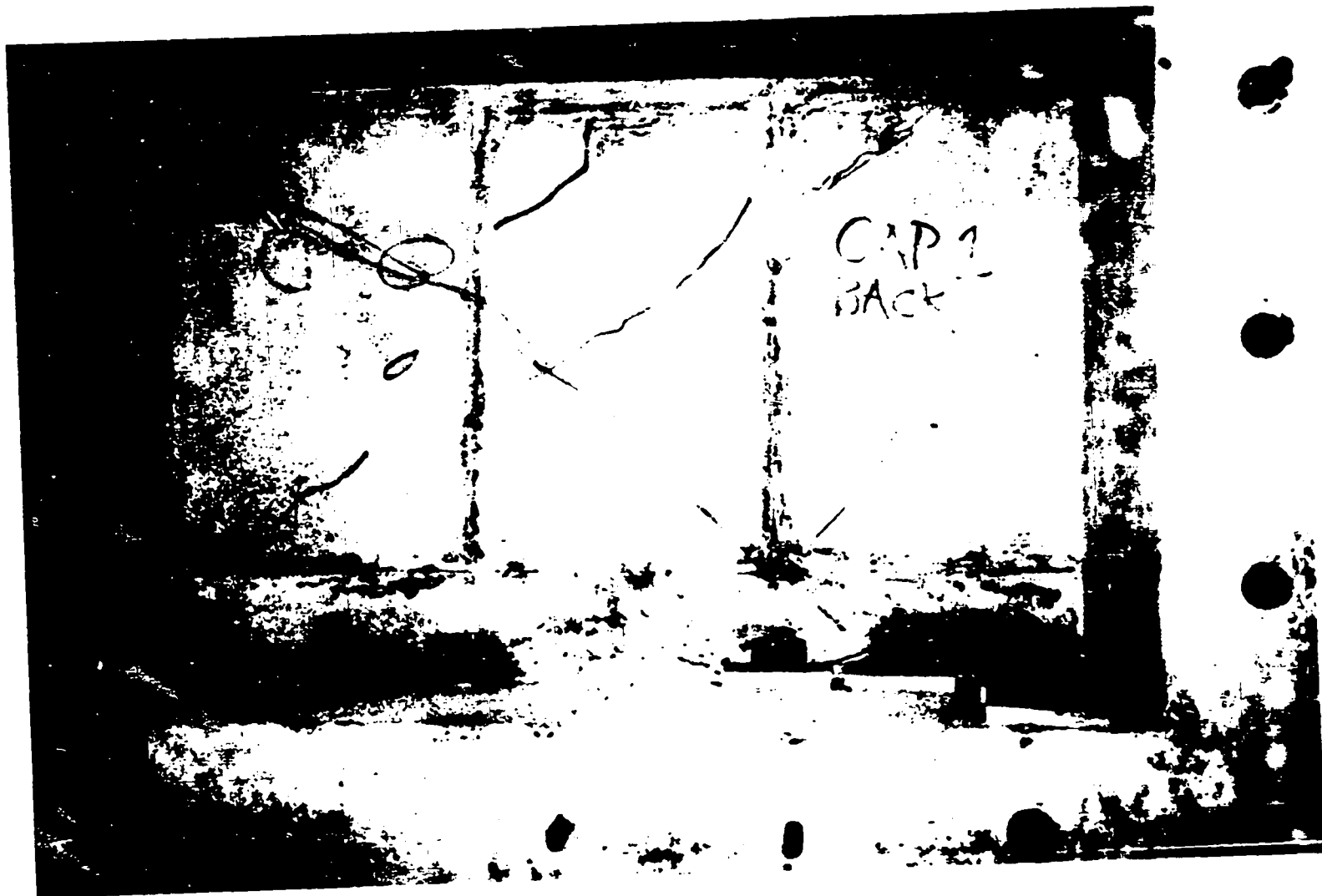


Fig. 15. CAP-1 crack pattern on back side of shear wall.

Air-flow measurements were made after the test structure was damaged. The cracking had a significant effect on the leakage of air through the shear wall. Both transient and steady-state airflow data were taken. A typical transient-pressure decay plot is illustrated in Fig. 16. For this test, the volume was charged to 12.0 psi with dry air. Table VII gives a summary of the pertinent information used to compute the average permeability for the transient test data shown in Fig. 16. Even though the presence of the cracks affects the theory behind Eq. (7), the average value of pseudo air permeability corresponding to the data is  $5.5 \times 10^{-12}$  in<sup>2</sup>.

Helium leak tests were performed to insure that the aluminum cover plate seals and fittings were not leaking. The leak-testing equipment verified that significant leakage was occurring through the shear cracks in the wall.

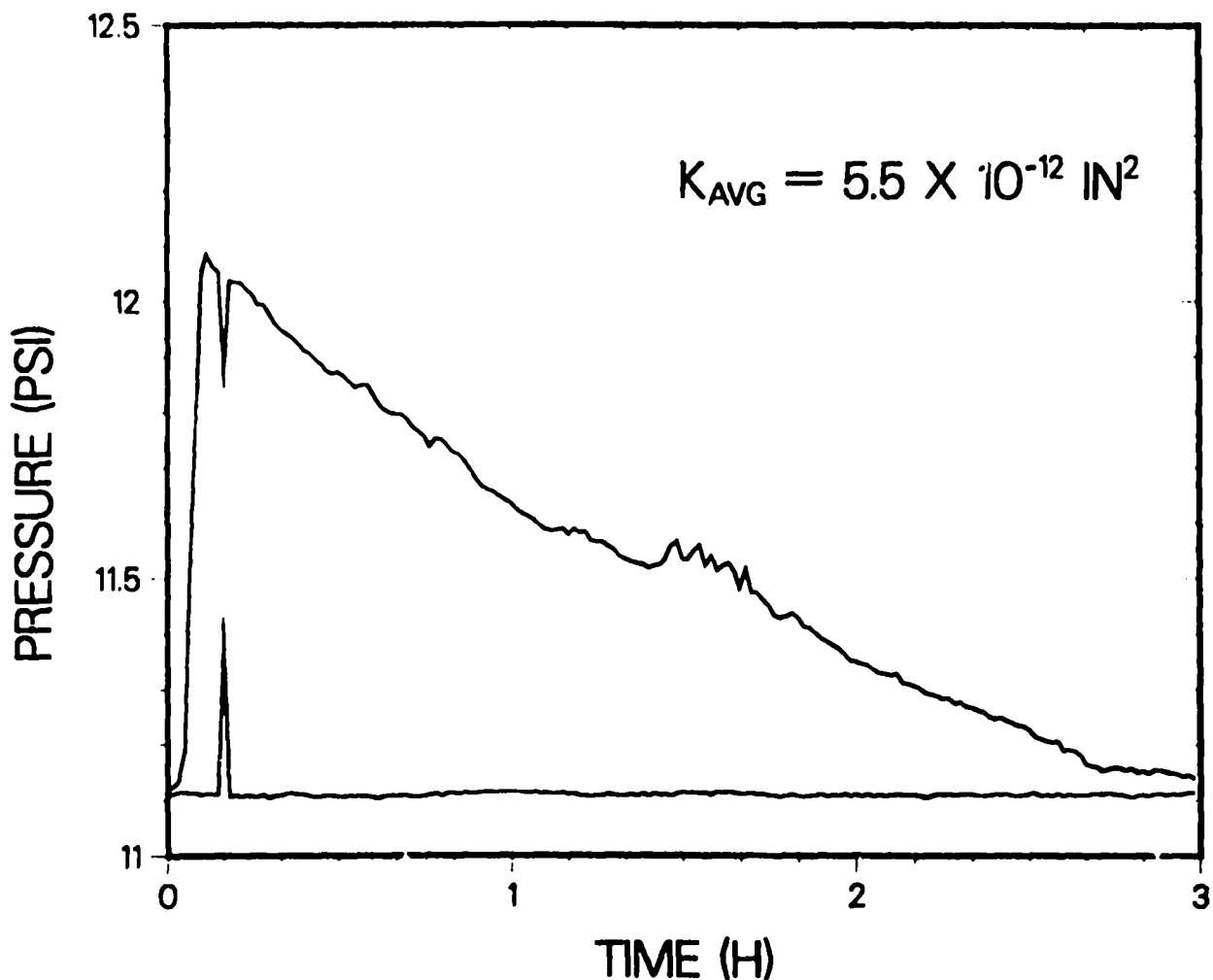


Fig. 16. Typical transient-pressure decay plot after test structure damage.

**TABLE VII**  
**TRANSIENT PERMEABILITY DATA FOR CRACKED CONCRETE SHEAR WALL**

Time (h)	P <sub>VOL</sub> (psi)	P <sub>ATM</sub> (psi)	P <sub>m</sub> (psi)	ΔP (psi)	Q <sub>m</sub> (ft <sup>3</sup> /h)	k (x10 <sup>-12</sup> in <sup>2</sup> )
0.0	12.074	11.112	-	-	-	-
0.5	11.807	11.105	11.94	0.268	0.34	3.5
1.0	11.574	11.112	11.69	0.233	0.30	4.4
1.5	11.512	11.114	11.54	0.062	0.08	1.6
2.0	11.317	11.110	11.41	0.195	0.26	7.2
2.5	11.180	11.111	11.25	0.137	0.18	11.1

A flowmeter was attached to the air-charging orifice on the aluminum cover plate. While approximately maintaining a constant pressure in the volume (see Fig. 17), the airflow through the shear wall was monitored for 168 hours. The steady airflow through the shear wall was 0.4 ft<sup>3</sup>/h. Table VIII gives a summary of the pertinent information used to compute the average permeability for the steady test data shown in Fig. 17. The pseudo air permeability corresponding to the steady flow rate and average pressure gradient is 4.7 x 10<sup>-12</sup> in<sup>2</sup>.

#### VIII. SUMMARY AND DISCUSSION

The objective of this study was to measure the air permeability in a reinforced concrete shear wall, both before and after seismic simulation loading. To accomplish this objective, a 6-in. shear wall test structure was fabricated with standard concrete mix and rebar materials. Four-thousand-psi compressive strength concrete and typical wall reinforcement ratios called out in the SNML Title I design were used in the construction of this structure. The concrete was placed, cured, and tested outside in an environment similar to that which an actual building will experience. The w/c ratio of the concrete was 0.35. Strength tests performed on test samples yielded an average compressive strength of 6086 psi and an average tensile strength of 516 psi.

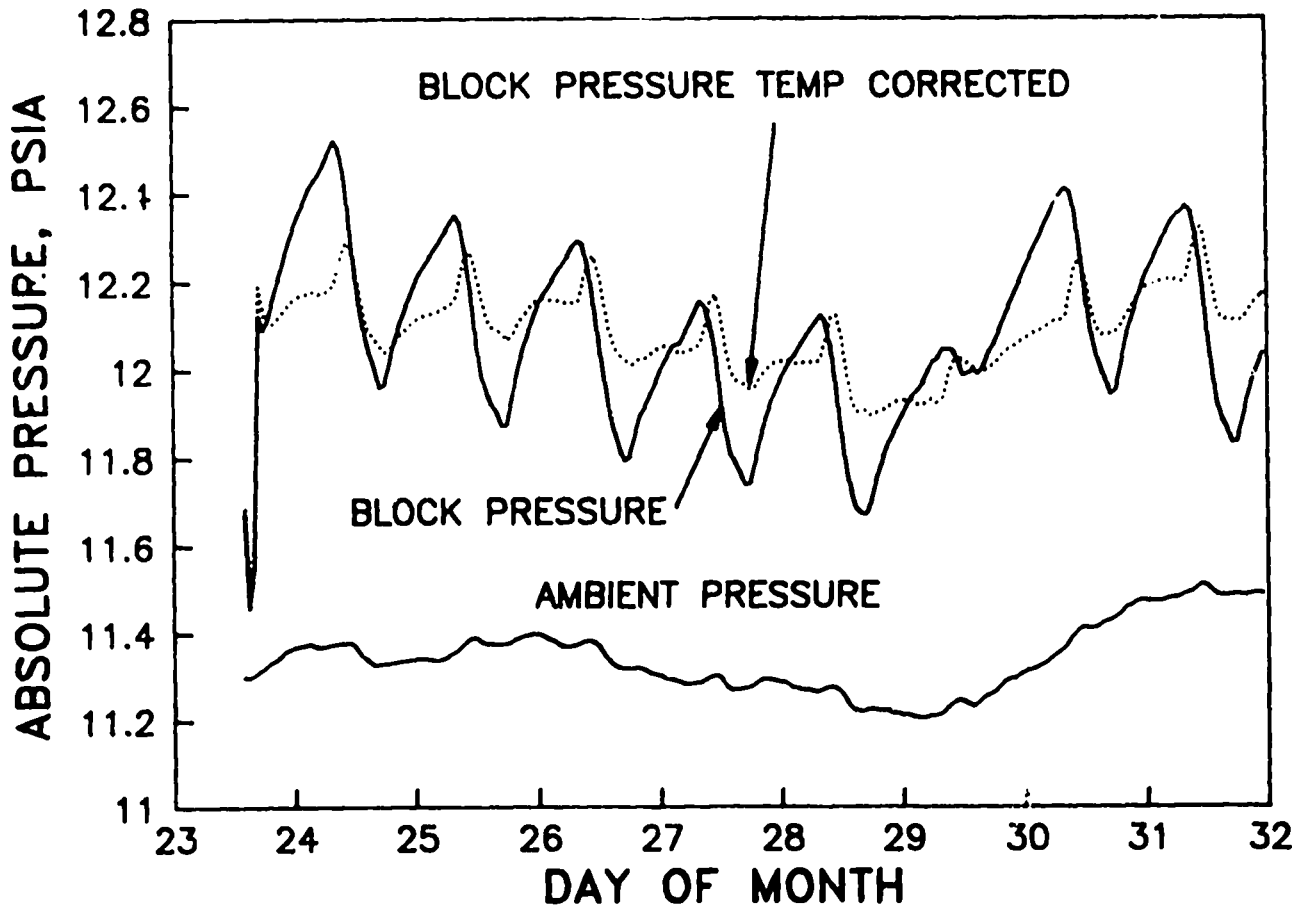


Fig. 17. Pressure variation over eight days during steady airflow test.

TABLE VIII  
STEADY PERMEABILITY DATA FOR CRACKED CONCRETE SHEAR WALL

Time (day)	P <sub>ATM</sub> (psi)	P <sub>VOL</sub> (psi)	T <sub>VOL</sub> (R)	k (x10 <sup>-12</sup> in <sup>2</sup> )
1.0	11.3555	12.2435	513.3	3.8
2.0	11.3355	12.1344	520.5	4.2
3.0	11.3964	12.0766	522.9	4.9
4.0	11.3071	11.9386	526.2	5.3
5.0	11.2930	11.8462	521.9	5.3
6.0	11.2162	11.8462	524.0	5.3
7.0	11.2962	12.1681	514.9	3.9
8.0	11.4700	12.1453	522.5	4.9

Air permeability measurements were made on the shear wall before static load cycling. One side of the test structure was pressurized with dry air to approximately 0.7 psig above atmospheric conditions. This pressure corresponds to the maximum pressure differentia caused by wind that was calculated for the SNML facility. The transient-pressure decay was monitored, and the intrinsic permeability was computed in accordance with Darcy's law. An air permeability of  $1.2 \times 10^{-13}$  in<sup>2</sup> was measured for this shear wall. A decontaminable coating system was also applied to the shear wall, but it did not have an impact on the measured permeability.

The air permeability measured before loading was compared to concrete permeability data published in the literature. Even for experiments performed on small laboratory specimens that were constructed and tested under very controlled conditions, published air permeabilities were found to vary by more than an order of magnitude. However, the results from the shear wall tests agreed best with the intrinsic permeability measurements performed by Dhir et al.<sup>11</sup> From the Dhir measurements, the air permeability of 0.47 w/c ratio concrete was  $4.0 \times 10^{-13}$  in<sup>2</sup> and the air permeability of 0.40 w/c ratio concrete was  $2.4 \times 10^{-13}$  in<sup>2</sup>. These two results show good agreement with the shear wall permeability measurements of  $1.2 \times 10^{-13}$  in<sup>2</sup>. As previously stated, the shear wall had a 0.35 w/c ratio concrete. Because permeability increases with increasing w/c ratio, the permeability results obtained in this investigation are consistent with those reported by Dhir.

Static load-cycle testing was used to simulate earthquake loading. The SNML Title 1 design showed that the actual structure would experience a peak NBSS of 190 psi during a DBE. The test structure was subjected to this same peak stress level during the static load cycling. Linear load-displacement response was observed when the structure was loaded to the maximum stress level. This response indicated that the shear wall was not damaged internally. Because the shear wall experienced no internal damage, the air permeability was not affected.

A single high-level load-cycle test resulted in damage (shear cracking) to the structure. The cracking was determined to have occurred at approximately 215-psi NBSS. Airflow measurements, taken after the structural damage had occurred, showed that the cracking had a significant effect on air leakage through the shear wall. The steady airflow through

the shear wall was measured to be 0.4 ft<sup>3</sup>/h. Even though the presence of the cracks affects the porous media assumptions used in the intrinsic permeability calculations, a pseudo air permeability was computed for the cracked concrete wall. The pseudo permeability corresponding to the steady flow rate and average pressure gradient measured was  $4.7 \times 10^{-12}$  in<sup>2</sup>. Thus, air permeability in the shear wall increased by a factor of 40 after the wall experienced shear cracking.

The results from this experiment can be used to estimate the air leakage through the exterior walls of the SNML facility in the event of ventilation system failure. A base-line leakage can be calculated by assuming that all of the exterior walls are undamaged. A maximum leakage can be calculated by using the measured air permeability associated with shear damage. Air leakage from the facility will only occur in wall areas exposed to a negative pressure gradient (i.e., internal air pressure exceeds the external air pressure). The maximum negative pressure gradient caused by wind loading on SNML, Bldg. 55-179 (see Appendix B) is -51.6 psf. The method used to compute the pressure loads caused by atmospheric winds was in accordance with standard Department of Energy (DOE) design practices. The negative pressure impacts only the side and leeward walls of a structure. Therefore, the total SNML wall area affected by the negative pressure gradient is approximately 22 800 ft<sup>2</sup>. Assuming 14-in.-thick walls, the base-line and maximum volume flow rates are 0.14 cfm and 5.4 cfm, respectively. Because air leakage is directly proportional to permeability and pressure gradient, a reduction in either of these variables will reduce the leakage rate.

A prototype experiment was successfully designed and performed to measure the air permeability in a reinforced concrete shear wall both before and after seismic simulation loading. Air permeability measurements made on the "as constructed" shear wall were in good agreement with concrete permeability values published in the literature. The shear wall deformation remained linear (i.e., no damage) when loaded up to the maximum-design shear stress level. As long as the structure exhibited linear load-displacement response, no variation in the value of air permeability was detected. At approximately 13% above the maximum-design shear stress, the shear wall cracked. It should be noted that, for a given load history, the onset of cracking is controlled by the concrete's

tensile strength. The compressive ultimate strength for the concrete used in this test structure was considerably higher than the Title I minimum design value and, hence, the tensile strength was also higher than might be expected for the actual structure. If the tensile strength of the actual SNML facility concrete was less, the structure might crack during the DBE. The air permeability in the shear wall increased by a factor of 40 as a result of the cracking.

## IX. RECOMMENDATIONS FOR FUTURE WORK

Further work needs to be done in order to adequately consider several issues arising from this study. The primary concerns are presented below in statements recommending future experimental activities.

1. Testing should be done on the shear wall test structure to assess the particulate filtering effectiveness of the cracked shear wall. This testing can be performed by substituting an aerosol (dioctylsebacate, DOS) for the dry air. For a base-line, the aerosol should also be used in permeability experiments before loading the structure.
2. The experiment described in this report was concerned with only that part of the structure loaded in shear. An out-of-plane bending test should also be performed. The bending stresses and shear stresses are the two significant stresses that would cause the concrete to crack and, hence, allow air leakage through the walls. The bending test should simulate the loading on the building wall by subjecting the test wall to a moment that will produce bending stresses in the wall. A test structure for the bending test could be similar to the shear wall test structure with the shear wall removed.
3. Because concrete is a statistical material and no two batches are identical, more experiments using the same test structure configuration and testing procedures should be performed. Four to six tests of both the shear and bending configurations should provide enough data to quantify the range of values that can be expected.

4. Shear wall test structures should be fabricated with a shear wall thickness larger than 6 in. Air permeability testing on these structures would be useful to address the issue of thickness scaling on both permeability and crack leakage measurements.
5. Test structures can easily be modified to study the effects of penetrations and construction joints on air leakage rates after seismic simulation loading.
6. The potential to retrofit critical facilities with impermeable liners can be addressed by installing candidate liner materials on structures that have been damaged and by performing air permeability experiments to measure liner effectiveness.

The results from the above recommended activities can be used in a study of existing facilities' confinement capabilities. First, any structure utilizing concrete walls for confinement barriers can be analyzed to calculate the stress levels that will result during the DBE and to determine if these levels are sufficient to cause cracking of the walls. Second, if seismic-induced cracking is credible, airflow calculations can be performed using the measured permeabilities for damaged structures to determine if increased leakage rates are a concern.

The test that was performed in this study showed that the effectiveness of using a concrete structure as a confinement barrier can be quantified. Even though the SNML Project at Los Alamos has been terminated, the results from this work are applicable to safety issues wherever concrete is used as a confinement barrier. Therefore, the information gained from performing the additional recommended experiments is directly applicable to addressing safety considerations throughout the DOE complex.

**APPENDIX A**

**CONCRETE TEST CYLINDERS LAB REPORT**



**WESTERN  
TECHNOLOGIES  
INC.**

2395 Washington Pl., e. N.E.  
Albuquerque, New Mexico 87113  
505/823-4488 • 821-2963 FAX

**LABORATORY REPORT**

Client Los Alamos National Laboratory #2-LFO-Q2131-1  
P.O. Box 1663, MS J576  
Los Alamos, NM 87545  
Attention: Mr. Lee Dalton

Job No  
Lab Invoice No 32400995  
Date of Report 11-5-90  
Reviewed By *Paul Peterson*

Project Concrete Permeability Experiment

Location Los Alamos, New Mexico

Material Specimen Concrete

Sampled By Client Date --

Source Test Box Unit

Submitted By Bill Whaley/WT Date 9-20-90

Test Procedure ASTM

Authorized By Client Date 9-20-90

**RESULTS**

SPLITTING TENSILE STRENGTH OF  
CYLINDRICAL CONCRETE SPECIMENS  
TESTED ON 10-02-90

<u>SPECIMEN</u>	<u>MAX. LOAD FORCE (lbs.)</u>	<u>SPLITTING TENSILE STRENGTH (psi)</u>
#1	49274	540
#2	54650	580
#3	67835	600
#4	61386	540
#5	58307	520

Copies to Client



**WESTERN  
TECHNOLOGIES  
INC.**

8305 Washington Place N.E.  
Albuquerque, New Mexico 87113  
(505) 823-4488 • 821-2963 FAX

**LABORATORY REPORT**

Client Los Alamos National Laboratory #2-LFO-Q2131-1  
P.O. Box 1663, MS J576  
Los Alamos, NM 87545  
Attention: Mr. Lee Dalton

Job No \_\_\_\_\_  
Lab /Invoice No 32400905  
Date of Report 11-5-90  
Reviewed By *Paul Peterson*

Project Concrete Permeability Experiment

Location Los Alamos, New Mexico

Material/Specimen Concrete

Source Test Box Unit

Test Procedure ASTM C39-86, C469-87a

Sampled By	Client	Date	--
Submitted By	Bill Whaley/WT	Date	9-20-90
Authorized By	Client	Date	9-20-90

**RESULTS**

**STRESS-STRAIN RESULTS**

FOR SPECIMENS TESTED ON 10-02-90

<u>Stress (psi)</u>	<u>Strain (in./in.)</u>	<u>Specimen: #6</u>	
237	.000047		
452	.000093		
682	.000139	E= 4.727 x 10 <sup>6</sup> psi	
909	.000186		
1135	.000232	<u>Maximum Load</u>	<u>Compressive Strength</u>
1360	.000287	188,640 lbs.	6670 psi
1588	.000333		

<u>Stress (psi)</u>	<u>Strain (in./in.)</u>	<u>Specimen: #7</u>	
248	.000047		
453	.000085		
683	.000178	E= 4.558 x 10 <sup>6</sup> psi	
909	.000240		
1135	.000279	<u>Maximum Load</u>	<u>Compressive Strength</u>
1362	.000341	181,260 lbs.	6410 psi
1588			

<u>Stress (psi)</u>	<u>Strain (in./in.)</u>	<u>Specimen: #8</u>	
258	.000047		
453	.000085		
683	.000132	E= 4.524 x 10 <sup>6</sup> psi	
909	.000178		
1135	.000232	<u>Maximum Load</u>	<u>Compressive Strength</u>
1362	.000279	173,730 lbs.	6150 psi
1588	.000341		

Notes to 3-Client



**WESTERN  
TECHNOLOGIES  
INC.**

8305 Washington Place, N.E.  
Albuquerque, New Mexico 87113  
(505) 823-4488 • 821-2965 FAX

**LABORATORY REPORT**

Client Los Alamos National Laboratory #2-LFO-02131-1  
P.O. Box 1663, MS 3576  
Los Alamos, NM 87545  
Attention: Mr. Lee Dalton

Job No  
Lab / Invoice No 32400991  
Date of Report 11-5-90  
Reviewed By *Paul Peterson*

Project Concrete Permeability Experiment  
Location Los Alamos, New Mexico

Material Specimen	Concrete	Sampled By	Client	Date	
Source	Test Box Unit	Submitted By	Bill Whaley/WT	Date	
Test Procedure	ASTM C39-86, C469-87a	Authorized By	Client	Date	

**RESULTS**

**STRESS-STRAIN RESULTS**

FOR SPECIMENS TESTED ON 10-02-90

<u>Stress (psi)</u>	<u>Strain (in./in.)</u>	<u>Specimen: #9</u>	
244	.000047		
452	.000093		
683	.000139	$E = 4.571 \times 10^6$ psi	
909	.000186		
1135	.000232	<u>Maximum Load</u>	<u>Compressive Strength</u>
1362	.000287	168,820 lbs.	5970 psi
1588	.000341		

<u>Stress (psi)</u>	<u>Strain (in./in.)</u>	<u>Specimen: #10</u>	
269	.000047		
452	.000085		
682	.000132	$E = 4.867 \times 10^6$ psi	
909	.000170		
1135	.000217	<u>Maximum Load</u>	<u>Compressive Strength</u>
1362	.000271	161,910 lbs.	5730 psi
1588	.000318		

<u>Stress (psi)</u>	<u>Strain (in./in.)</u>	<u>Specimen: #11</u>	
269	.000047		
453	.000085		
682	.000124	$E = 4.867 \times 10^6$ psi	
909	.000170		
1135	.000217	<u>Maximum Load</u>	<u>Compressive Strength</u>
1362	.000263	175,500 lbs.	6210 psi
1588	.000318		

Copies to 3-Client



**WESTERN  
TECHNOLOGIES  
INC.**

8405 Valbuena Pl. N.E.  
Albuquerque, New Mexico 87113  
505/823-4488 • 821-2963 FAX

**LABORATORY REPORT**

Client: Los Alamos National Laboratory #2-1FO-02131-1  
P.O. Box 1663, MS 576  
Los Alamos, NM 87545  
Attention: Mr. Lee Dalton

Job No.  
Lab Invoice No. 33400995  
Date of Report 11-5-90  
Reviewed By *Paul Johnson*

Project: Concrete Permeability Experiment  
Location: Los Alamos, New Mexico

Material Specimen	Concrete	Sampled By	Client	Date	--
Source	Test Box Unit	Submitted By	Bill Whaley/ET	Date	9-20-90
Test Procedure	ASTM C39-86, C469-87a	Authorized By	Client	Date	9-20-90

**RESULTS**

**STRESS-STRAIN RESULTS**

FOR SPECIMENS TESTED ON 10-02-90

<u>Stress (psi)</u>	<u>Strain (in./in.)</u>	<u>Specimen: #12</u>	
251	.000047		
453	.000085		
682	.000139	$E=4.674 \times 10^6$ psi	
909	.000178		
1135	.000232	<u>Maximum Load</u>	<u>Compressive Strength</u>
1362	.000279	165,310 lbs.	5850 psi
1588	.000333		

<u>Stress (psi)</u>	<u>Strain (in./in.)</u>	<u>Specimen: #13</u>	
248	.000047		
453	.000085		
682	.000139	$E=4.815 \times 10^6$ psi	
909	.000178		
1135	.000225	<u>Maximum Load</u>	<u>Compressive Strength</u>
1362	.000271	163,710 lbs.	5790 psi
1588	.000325		

<u>Stress (psi)</u>	<u>Strain (in./in.)</u>	<u>Specimen: #14</u>	
233	.000047		
453	.000093		
682	.000147	$E=4.494 \times 10^6$ psi	
909	.000194		
1135	.000248	<u>Maximum Load</u>	<u>Compressive Strength</u>
1362	.000294	179,930 lbs.	6360 psi
1588	.000349		

Copies to 3-Client



**WESTERN  
TECHNOLOGIES  
INC.**

2305 Washington Place, N.E.  
Albuquerque, New Mexico 87113  
(505) 823-4488 • 821-2963 FAX

LABORATORY REPORT

Client Los Alamos National Laboratory #2-LFO-Q2131-1  
P.O. Box 1663, MS J576  
Los Alamos, NM 87545  
Attention: Mr. Lee Dalton

Job No  
Lab /Invoice No 32400995  
Date of Report 11-5-90  
Reviewed By *David Robinson*

Project Concrete Permeability Experiment  
Location Los Alamos, New Mexico

Material Specimen	Concrete	Sampled By	Client	Date	--
Source	Test Box Unit	Submitted By	Bill Whaley/WT	Date	9-20-90
Test Procedure	ASTM C39-86, C469-87a	Authorized By	Client	Date	9-20-90

**RESULTS**

**STRESS-STRAIN RESULTS  
FOR SPECIMENS TESTED ON 10-02-90**

<u>Stress (psi)</u>	<u>Strain (in./in.)</u>	<u>Specimen: #15</u>	
251	.000047		
453	.000093		
682	.000147	E=4.110 x 10 <sup>6</sup> psi	
909	.000194		
1135	.000248	<u>Maximum Load</u>	<u>Compressive Strength</u>
1362	.000294	161,700 lbs.	5720 psi
1538	.000349		

Copies to 1-Client

**APPENDIX B**

**NEGATIVE WIND PRESSURE CALCULATION  
SNML, BLDG 55-179**

## B.1 SCOPE

The following text describes the ANSI A58.1<sup>26</sup> approach for calculating the negative pressure gradient caused by wind loading on SNML, Bldg 55-179.

## B.2 BACKGROUND

Wind flow around a structure causes varying pressures on the wall surfaces and roof. The dynamic pressure on the windward surfaces is greater than the dynamic pressure on the sides, leeward, and roof areas. This phenomenon results in a positive pressure acting toward the structure on the windward side and a negative pressure, or suction force, acting on the other areas. Pressure inside the structure is not affected by the wind when the structure is sealed. The negative pressure on the sides, leeward, and roof areas results in a positive pressure gradient between the inside and outside of the structure, creating a potential for air leakage through the structure to the outside.

The Bernoulli equation mathematically describes the change in pressure caused by wind on a structure. The equation basically states that, in a streamline, pressure decreases as velocity increases. As air flows towards a structure along a streamline, the building forces the flow to alter its path and go around the structure. This change in flow path increases the distance that the air must travel and forces an increase in velocity. As a result, the corners of the roof and walls experience the greatest change in velocity and, hence, the lowest pressures.

## B.3 STRATEGY

The analytical procedures described in ANSI A58.1 and demonstrated in the Wind Load Provisions (WLP) Guide<sup>27</sup> for components and cladding are used to calculate the pressure loads caused by atmospheric winds.

The components and cladding approach allows one to determine the maximum wind load conditions. The governing equation for calculating the design pressure,  $p$ , is

$$p = q_h(GC_p) - q_h(GC_{pi}) \quad (\text{Ref. 26, Table 4, } h < 60 \text{ ft}) ,$$

where

$q_h$  = velocity pressure (psf) at the mean roof height,  $h$  (ft),

$q_h = 0.00256K_h(IV)^2$  (Ref. 27, Eq. 2-4),

$K_h$  = velocity pressure coefficient at height  $h$   
(Ref. 26, Table 6),

$I$  = importance factor  
(Ref. 26, Table 5),

$V$  = basic wind speed (mph)  
(Ref. 28, Table 5-3),

$GC_p$  = gust response factor times the external pressure coefficient  
(Ref. 26, Fig. 3), and

$GC_{pi}$  = gust response factor times the internal pressure coefficient  
(Ref. 26, Table 9).

The overall analytical procedure involves (1) selecting an exposure category, (2) determining  $V$ , the basic wind speed, (3) calculating  $q_h$ , the velocity pressure, and (4) calculating  $p$ , the design wind pressure.

#### B.4 CALCULATION SUMMARY

All elevation/siting views (N, S, E, W) were considered in determining the worst case negative pressure gradient. The southern exposure was found to give the largest negative value and is detailed below.

- (1) Exposure C. Required by ANSI A58.1 when using components and cladding approach for structures less than 60 ft.

(2) Per UCRL-15910, the Los Alamos National Laboratory has a high hazard wind speed of 107 mph. This wind speed has a 0.0001 annual probability of exceedance.

(3)  $h = 52$  ft,  
 $l = 1.07$ ,  
 $K_h = 1.14$ , and  
 $q_h = 0.00256(1.14)[(1.07)(107)]^2 = 38.25$  psf.

(4)  $a = 0.4h = 20.8$  ft,  
 $A = 20.8(52) = 1081.6$  ft<sup>2</sup>,  
 $GC_p = -1.1$ ,  
 $GC_{pi} = 0.25$ , and  
 $p = 38.25(-1.1) - 38.25(0.25) = -51.6$  psf.

## B.5 CONCLUSION

The worst case negative pressure gradient caused by wind loading on the SNML facility, Bldg 55-179 is -51.6 psf. This value was determined by considering normal wind incidence on all four siting exposures.

## REFERENCES

1. *Handbook of Concrete Engineering*, M. Fintel, Ed. (Van Nostrand Reinhold, New York), 1974, pp.176-177.
2. J. W. Figg, "Method of Measuring the Air Permeability of Concrete," *Magazine of Concrete Research* **25** (85), 213-218 (1973).
3. R. Cather et al., "Improvements to the Figg Method for Determining the Air Permeability of Concrete," *Magazine of Concrete Research* **36** (129), 241-245 (1984).
4. Y. Kasai, I. Matsui, and M. Nagano, "On Site Rapid Air Permeability Test for Concrete," in *In Situ/Nondestructive Testing of Concrete* V. M. Malhotra, Ed., SP-82 (American Concrete Institute, Detroit, Michigan, 1984), pp. 525-541
5. A. J. Hansen, N.S. Ottosen, and C. G. Petersen, "Gas-Permeability of Concrete In Situ: Theory and Practice," in *In Situ/Nondestructive Testing of Concrete* V. M. Malhotra, Ed., SP-82 (American Concrete Institute, Detroit, Michigan, 1984), pp. 543-556.
6. Y. Kasai, I. Matsui, and M. Nagano, "Relationship Between Carbonation and Air Permeability of Concrete," *Transactions of the Japan Concrete Institute* **6**, 171-178 (1984).
7. Y. Kasai, I. Matsui, and T. Aoki, "Long Term Changes of Air Permeability by Rapid Test," *Transactions of the Japan Concrete Institute* **8**, 145-152 (1986).
8. S. Nagataki and I. Ujike, "Air Permeability of Concretes Mixed with Fly Ash and Condensed Silica Fume," in *Fly Ash, Silica Fume, Slag, and Natural Pozzolans in Concrete* V. M. Malhotra, Ed., SP-91 (American Concrete Institute, Detroit, Michigan, 1986), pp. 1049-1068.
9. R. Martialay, "Concrete Air Permeability-Age Effects on Concrete," in *Concrete Durability, Vol. 1* SP-100 (American Concrete Institute, Detroit, Michigan, 1987), pp. 335-350.
10. K. Schonlin and H. K. Hilsdorf, "Permeability as a Measure of Potential Durability of Concrete-Development of a Suitable Test Apparatus," in *Permeability of Concrete* SP-108 (American Concrete Institute, Detroit, Michigan, 1988), pp. 99-115.

11. R. K. Dhir, P. C. Hewlett, and Y. N. Chan, "Near Surface Characteristics of Concrete: Intrinsic Permeability," *Magazine of Concrete Research* **41** (147), 87-97 (1989).
12. Y. Nojiri and K. Fujii, "Utilization of Cement Concrete as an Evaporator Shell Material," *Desalination* **19**, 45-54 (1976).
13. L. F. Epstein, T. C. Hall Jr., and S. E. Mills, "Preliminary Gas Permeation Measurements on Plastics for Use as Concrete Containment Vessel Liners," *Nuclear Engineering and Design* **8**, 345-359 (1968).
14. Chr. Mayrhofer, W. Korner, and W. Brugger, "Gas Impermeability of Reinforced Concrete Slabs Supported on Four Sides. Part 2," Foreign Technology Division Wright-Patterson AFB report FTD-ID(RS) T-0085-88 (May 1988).
15. American Concrete Institute Committee 318, *Building Code Requirements for Reinforced Concrete* (American Concrete Institute, Detroit, Michigan, 1983).
16. "Standard Test Method for Slump of Portland Cement Concrete," *Annual Book of ASTM Standards*, Roberta A. Prieman-Storer, Ed. (American Society for Testing and Materials, Philadelphia, Pennsylvania, 1985), Vol. 4.02, C143-78, pp. 109-112.
17. "Method of Sampling Freshly Mixed Concrete," *Annual Book of ASTM Standards*, Roberta A. Prieman-Storer, Ed. (American Society for Testing and Materials, Philadelphia, Pennsylvania, 1985), Vol. 4.02, C172-82, pp. 133-135.
18. "Standard Method of Making and Curing Concrete Specimen in the Field," *Annual Book of ASTM Standards*, Roberta A. Prieman-Storer, Ed. (American Society for Testing and Materials, Philadelphia, Pennsylvania, 1985), Vol. 4.02, C31-84, pp. 5-10.
19. "Standard Test Method for Compressive Strength of Cylindrical Concrete Specimen," *Annual Book of ASTM Standards*, Roberta A. Prieman-Storer, Ed. (American Society for Testing and Materials, Philadelphia, Pennsylvania, 1985), Vol. 4.02, C39-84, pp. 24-29.

20. "Standard Test Method for Static Modulus of Elasticity and Poisson's Ratio of Concrete in Compression," *Annual Book of ASTM Standards*, Roberta A. Prieman-Storer, Ed. (American Society for Testing and Materials, Philadelphia, Pennsylvania, 1985), Vol. 4.02, C469-83, pp. 303-307.
21. "Standard Test Method for Splitting Tensile Strength of Cylindrical Concrete Specimens," *Annual Book of ASTM Standards*, Roberta A. Prieman-Storer, Ed. (American Society for Testing and Materials, Philadelphia, Pennsylvania, 1985), Vol. 4.02, C496-85, pp. 335-339.
22. P. Huovinen, "Air-Permeability of Concrete," *Nordic Concrete Research* 1, 1-17 (December 1982).
23. C. R. Farrar, J. G. Bennett, W. E. Dunwoody, and W. E. Baker, "Static Load Cycle Testing of a Low-Aspect-Ratio Six-Inch Wall, TRG-Type Structure TRG-4-6 (1.0, 0.25)," Los Alamos National Laboratory report LA-11422-MS, NUREG/CR-5222 (June 1989).
24. C. R. Farrar, J. G. Bennett, W. E. Dunwoody, and W. E. Baker, "Static Load Cycle Testing of a Low-Aspect-Ratio Four-Inch Wall, TRG-Type Structure TRG-5-4 (1.0, 0.56)," Los Alamos National Laboratory report LA-11739-MS, NUREG/CR-5487 (November 1990).
25. C. R. Farrar, J. G. Bennett, W. E. Baker, and W. E. Dunwoody, "Static Load Cycle Testing of a Very Low-Aspect-Ratio Six-Inch Wall, TRG-Type Structure TRG-6-6 (0.27, 0.50)," Los Alamos National Laboratory report LA-11796-MS, NUREG/CR-5533 (November 1990).
26. "Minimum Design Loads for Buildings and Other Structures," ANSI A58.1-1982 (American National Standards Institute, Inc., New York, 1982).
27. "Guide to the Use of the Wind Load Provisions of ANSI A58.1," Kishor C. Mehta, Ed. (Institute for Disaster Research, Texas Tech University, Lubbock, Texas, 1988).
28. R. P. Kennedy, et al., "Design and Evaluation Guidelines for Department of Energy Facilities Subjected to Natural Phenomena Hazards," Lawrence Livermore National Laboratory report UCRL-15910 (June 1990).